Journal of Theoretical Biology 515 (2021) 110562

Contents lists available at ScienceDirect

Journal of Theoretical Biology

journal homepage: www.elsevier.com/locate/yjtbi

Mathematical assessment of the impact of human-antibodies on sporogony during the within-mosquito dynamics of *Plasmodium falciparum* parasites

Miranda I. Teboh-Ewungkem [a], Woldegebriel Assefa Woldegerima [b,c,*], Gideon A. Ngwa [d]

[a] Department of Mathematics, Lehigh University, Bethlehem, PA 18015, USA
[b] Department of Mathematics and Applied Mathematics, University of Pretoria, Hatfield, 0028 Pretoria, South Africa
[c] Department of Mathematics, Mekelle University, P.O. Box 231, Mekelle, Ethiopia
[d] Department of Mathematics, University of Buea, P.O. Box 63, Buea, Cameroon

ARTICLE INFO

Article history:
Received 4 July 2020
Revised 25 November 2020
Accepted 14 December 2020
Available online 24 December 2020

Keywords:
Malaria parasites
Within-mosquito
Sporogony
Gametogenesis
Human antibodies
Transmission blocking
Mathematical modelling

ABSTRACT

We develop and analyze a deterministic ordinary differential equation mathematical model for the within-mosquito dynamics of the *Plasmodium falciparum* malaria parasite. Our model takes into account the action and effect of blood resident human-antibodies, ingested by the mosquito during a blood meal from humans, in inhibiting gamete fertilization. The model also captures subsequent developmental processes that lead to the different forms of the parasite within the mosquito. Continuous functions are used to model the switching transition from oocyst to sporozoites as well as human antibody density variations within the mosquito gut are proposed and used. In sum, our model integrates the developmental stages of the parasite within the mosquito such as gametogenesis, fertilization and sporogenesis culminating in the formation of sporozoites. Quantitative and qualitative analyses including a sensitivity analysis for influential parameters are performed. We quantify the average sporozoite load produced at the end of the within-mosquito malaria parasite's developmental stages. Our analysis shows that an increase in the efficiency of the ingested human antibodies in inhibiting fertilization within the mosquito's gut results in lowering the density of oocysts and hence sporozoites that are eventually produced by each mosquito vector. So, it is possible to control and limit oocysts development and hence sporozoites development within a mosquito by boosting the efficiency of antibodies as a pathway to the development of transmission-blocking vaccines which could potentially reduce oocysts prevalence among mosquitoes and hence reduce the transmission potential from mosquitoes to human.

1. Introduction

The life cycle of *Plasmodium* parasites within a female *Anopheles* mosquito (the malaria vector) commences with the ingestion of mature (late stage) gametocytes by the mosquito during a blood meal from an infectious human. Once these malaria parasites are ingested by mosquito, they follow a prescribed developmental pathway leading to the formation of a new brood of the form the parasites, called sporozoites, in the mosquito that can be passed on to humans once the mosquito blood feeds on another human. The length of time required for the development of the parasite in the mosquito (the extrinsic incubation period) varies within and among *Plasmodium* species and is temperature dependent (Baton and Ranford-Cartwright, 2005; CDC, 2015).

The life cycle of *Plasmodium* commences with the ingestion of male and female *Plasmodium* gametocytes with a blood meal taken by a female *Anopheles* mosquito from an infectious human. Within the lumen of the mosquito's midgut, activation leading to gametogenesis occurs with each male gametocytes producing up to 8 micro (male) gametes and female gametocytes each producing 1 macro (female) gamete (Baton and Ranford-Cartwright, 2005; Mueller et al., 2010). About two hours after the blood meal, fertilization takes place with fusion between male and female gametes, producing zygotes (Baton and Ranford-Cartwright, 2005; Bennink et al., 2016; Dhar and Kumar, 2003). The zygotes undergo meiosis and develop into the motile ookinetes, which further develop into oocysts. Oocysts then undergo multiple rounds of asexual replication resulting in the production of sporozoites – *a process called sporogony*. After completion of the sporozoite formation process,

* Corresponding author at: Department of Mathematics and Applied Mathematics, University of Pretoria, Hatfield, 0028 Pretoria, South Africa.
E-mail address: wa.woldergerima@up.ac.za (W.A. Woldegerima).

https://doi.org/10.1016/j.jtbi.2020.110562
0022-5193/

thousands of sporozoites are waiting in the oocyst to be released into the mosquito hemolymph (Aly et al., 2009; Krettli and Miller, 2001). About 10^3—10^4 sporozoites can be released per bursting oocyst (Baton and Ranford-Cartwright, 2005; Beier, 1998; Teboh-Ewungkem and Yuster, 2010; Teboh-Ewungkem et al., 2010). Sporozoites released in the mosquito hemocele then invade the salivary glands of the mosquito, where they mix with saliva ready to be injected into the next vertebrate host during a blood meal.

The life cycle within a human host commences when an infected female *Anopheles* mosquito injects sporozoites into the human's skin during feeding. Sporozoites enter the human's blood stream and are carried to the liver, where they infect liver cells, multiply within liver cells and the parasites develop into (hepatic) schizonts, which eventually rupture, releasing thousands of free merozoites into the human bloodstream (Aly et al., 2009; Baton and Ranford-Cartwright, 2005; Beier, 1998; Dhar and Kumar, 2003; Mueller et al., 2010; Tavares, 2013; Teboh-Ewungkem and Yuster, 2010); on average 30,000 merozoites (Gazzinelli et al., 2014). Released merozoites invade and infect the erythrocytes (RBCs) or die. The merozoites undergo asexual multiplication and develop into schizonts which eventually will rupture releasing 4–36 daughter merozoites (Kaushal et al., 1980), depending on the *Plasmodium* species, and invade fresh RBC to continue the asexual life cycle. Repeated cycles lead to depletion of healthy red blood cells thereby causing illness and potential death if not treated. During invasion of healthy erythrocytes by free merozoites, a proportion of merozoites inside the red blood cells switch to produce gametocyte stages-*the sexual stages infective to the mosquito vectors* (Kaushal et al., 1980).

In malaria regions, an infected human develops both cellular and humoral immune responses against pre-erythrocytic stages in the liver, erythrocytic and sexual stages parasites, with the immune responses that are acquired (adaptive) becoming increasingly well defined with repeated exposure to the parasite (Arévalo-Herrera et al., 2011; Churcher et al., 2012; Delves et al., 2018; Holz et al., 2016; Kaslow, 1993; Kengne-Ouafo et al., 2019; Klein et al., 2008; Manore et al., 2019; Teboh-Ewungkem et al., 2014). These acquired immunity can either inhibit parasitization of healthy liver cells by sporozoites, parasitization of healthy red blood cells by merozoites, reduction of parasitemia by elimination of merozoites and infected red blood cells or inhibition of the formation and/or maturation of gametocytes, Augustine et al. (2009), Bousema et al. (2011), Holz et al. (2016), Kengne-Ouafo et al. (2019), Ngwa et al. (2020), Woldegerima et al. (2019). Its been reported that naturally acquired antibodies to the sexual stages of the malaria parasites within a human can interfere with the transmission of *Plasmodium* by female mosquitoes, where fertilization of gametes in the mosquitoes midgut can be blocked by cytokines and specific antibodies (Arévalo-Herrera et al., 2011; Sinden, 2010). That is, two major processes can mediate transmission-blocking immunity: (i) non-specific factors, such as cytokines that inhibit transmissibility of gametocytes to mosquitoes; and (ii) specific factors, which are naturally boosted by infection, whereby antibodies that can specifically recognize sexual stage parasite surface proteins block development of the parasite in the mosquito midgut (Kaslow, 1993). Two broad categories of parasite-derived molecules associated to transmission blocking immunity are identified in Delves et al. (2018): immunity against proteins naturally boosted by infection expressed in gametocytes and gametes; immunity against proteins expressed in mosquito-only parasite stages – gametes, zygotes and ookinetes. The latter are never expressed in humans and thus free from human immune pressures. Alternatively, when gametocytes that are not transmitted to mosquitoes die, which is a vast majority of them, they release intracellular proteins/antigens into the host circulation which could be boosted following immunization with a vaccine targeted to some gametocyte antigens, providing long-lasting transmission-blocking immunity. These antigens would then be processed and presented for recognition, eventually evoking humoral immune responses which can be picked up together with mature gametocytes in a blood meal taken by a feeding female mosquito (Delves et al., 2018; Kengne-Ouafo et al., 2019). These acquired antibodies can substantially or completely block gametogenesis and fertilization in the mosquito (Baton and Ranford-Cartwright, 2005; Bousema et al., 2011; Bousema et al., 2007; Kengne-Ouafo et al., 2019; McQueen et al., 2013; Ngwa et al., 2020) subsequently reducing zygote production in the mosquito's midgut. If ingested gametocytes fail to start the next phase of development within the mosquito's midgut, or fail to produce oocysts and hence sporozoites, transmission is considered unsuccessful. This is the essence of transmission reducing immunity (TRI) and serves as a basis for the development of transmission blocking vaccines (TBV) against parasite stages in the mosquito (Churcher et al., 2012; Kengne-Ouafo et al., 2019). In this manuscript, effective antibody load/efficiency that would be considered as successful in inhibiting transmission would be a load that would result in the production of less than one oocyst.

Factors such as the density of the gametocytes ingested as well as their viability, the presence or lack of human antibodies in the ingested blood meal are all important factors play an important role here (Bousema et al., 2011; Gardiner et al., 2015; Teboh-Ewungkem and Wang, 2012; Teboh-Ewungkem and Yuster, 2010; Teboh-Ewungkem and Yuster, 2016; Teboh-Ewungkem et al., 2010).

The search for vaccines against malaria parasites is ongoing and has been for decades with different vaccines aimed at either the pre-erythrocytic stages, the blood stages or the mosquito stages of the malaria parasite (Ballou, 2009; Draper et al., 2018; Graves and Gelband, 2016; Hill, 2011; Kuehn and Pradel, 2010; Laurens, 2020; Nunes et al., 2014; Sauerwein and Bousema, 2015; MVI PATH, 2017; Valupadasu and Mateti, 2012; WHO, 2020). For example, there are pre-erythrocytic vaccines aimed at inhibiting sporozoite infection, with the leading candidate being the *RTS,S/AS*01, Ballou (2009), Draper et al. (2018), Laurens (2020), MVI PATH (2017), Valupadasu and Mateti (2012), which has demonstrated that it can reduce malaria as well as severe life-threatening malaria in African children. Other pre-erythrocytic vaccines target merozoite invasion, inhibiting the process via antibody activities, seeking to prevent the progression of liver stage infections to blood stage infections. Yet again, others target infected hepatocytes, killing them via T cell responses (Doumbo et al., 2018; Draper et al., 2018). Blood stage parasite vaccines aim to prevent infected red blood cell (IRBC)-mediated pathology, conferring protection that would reduce the severity of malaria episodes and/or parasitemia (Doumbo et al., 2018; Draper et al., 2018).

There is hope of developing a vaccine that can either trigger an immune response that can defend against the very first stages of parasitemia in humans, at the liver level (like the, or against blood stage parasites or that interrupts malaria transmission from humans to mosquitoes, or target the sexual sporogonic-mosquito (SSM) stages of the parasite in mosquitoes. Liver stage vaccines, presumably act through T cell responses and possibly antibodies and prevent progression of liver stage infections to blood stage parasitemia, Doumbo et al. (2018). Vaccines against the mosquito parasite stages aim at disrupting the within-mosquito parasite life cycle (Chaturvedi et al., 2016; Draper et al., 2018; Doumbo et al., 2018), with the goal of reducing or eliminating the transmission potential of the parasites from mosquitoes to humans. There vaccines are generally termed Transmission Blocking Vaccines (TBV). With transmission blocking vaccines (TBV), the idea is that a vaccinated human will transfer induced antibody-mediated immunity

to a feeding mosquito during a successful blood meal and these antibodies can serve to slow or block within-mosquito parasite development eventually slowing or blocking transmission of the parasites (sporozoites) by the mosquito to another individual (Biswas, 2017; Carter, 2001; Doumbo et al., 2018; Kapulu et al., 2010). Various transmission blocking vaccine (TBV) candidates are currently under investigation such as Pfs25, Pfs28, Pfs230, Pfs48/45, Pfs47, HAP2 and AnANP1 (Acquah et al., 2019; Chaturvedi et al., 2016; Draper et al., 2018; de Jong et al., 2020). Candidates Pfs230 and Pfs48/45 are antigens that begin their expression within a human host in the intracellular gametocytes and induce antibody responses in humans that are naturally exposed, meanwhile Pfs25 and Pfs28 are antigens that begin their expression in the mosquito vector in the extracellular gametocytes. Among the aforementioned TBV candidates, Pfs230, Pfs48/45 and Pfs25, are currently under development and aim to disrupt the fertilization process, inhibiting zygote production (Acquah et al., 2019). The leading candidate is Pfs25, and it is in phase I clinical trials, Chaturvedi et al. (2016), where in early field clinical trials, a short-lived vaccine-induced antibody functional response was demonstrated in mosquito-feeding assays. Current development focuses on improving the methods and vaccine delivery systems in order to generate long-lasting immune responses (Chaturvedi et al., 2016; Doumbo et al., 2018).

As for the candidate Pfs28, antibodies against it were not found to be effective although they enhanced the transmission blocking activity of the antibodies against Pfs25. The TBV candidates Pfs47, HAP2 and AnANP1 are recent discoveries and they are all expressed by within-mosquito parasites: Pfs47 and HAP2 target zygote development while AnANPI is a mosquito midgut antigen (Acquah et al., 2019).

Efficient control and management of malaria and related problems require that more economical and reliable methods be used (Ngwa and Shu, 2000; Teboh-Ewungkem et al., 2013). Development of new control strategies would entail a good understanding of the mechanisms that characterise malaria transmission and the associated parameters. More realistic and robust mathematical models can play a role in forecasting and designing of new strategies in Investigating the dynamics of the different developmental stages of the *Plasmodium falciparum* parasite within the mosquito. Even though several articles exist on mathematical modelling of the population dynamics of the malaria vector or the vector itself, (see, for example, Anguelov et al. (2012), Ngwa (2006), Ngwa and Shu (2000), Ngwa and Teboh-Ewungkem (2016)), the literature on mathematical models for the within mosquito-host dynamics of the malaria parasites is scanty. To the best of our knowledge, the first such model is found in the Teboh-Ewungkem and Yuster (2010); Teboh-Ewungkem et al., 2010, in which the authors developed a model that simulates the within-mosquito dynamics of *Plasmodium falciparum* in an *Anopheles* mosquito by taking blood meal as input and the final sporozoite load as output. The model in Teboh-Ewungkem and Yuster (2010) and Teboh-Ewungkem et al. (2010) was subsequently used in Teboh-Ewungkem and Wang (2012) and Teboh-Ewungkem and Yuster (2016) to understand the dynamic relationship between gametocyte sex-ratios, male gametocyte fecundity and size of ingested gametocytes. Another paper worth mentioning is that by Chaturvedi and Prosper (2017) wherein the authors extended the work of Teboh-Ewungkem and Yuster (2010) and Teboh-Ewungkem et al. (2010) to a stochastic formulation and used it to study how the diversity of the within-human parasite forms picked up by a feeding mosquito relates to the subsequent diversity of the mosquito parasite forms that exit the mosquito. None of the aforementioned works quantified the impact ingested human antibodies can have on the development and size of the within-mosquito parasite forms, a task we aim to achieve in this manuscript. In so doing, we extend the model in Teboh-Ewungkem and Yuster (2010) and Teboh-Ewungkem et al. (2010) by incorporating the potential impact of ingested human antibodies on the within-mosquito parasite developmental and transition processes. The model, a system of nonlinear continuous-time ordinary differential equations, is then used to quantify oocysts density and sporozoites load that can be produced by an infected mosquito at the end of the sporogonic cycle under human adaptive immunity effects. We note here that much s repeated from Teboh-Ewungkem and Yuster (2010) and Teboh-Ewungkem et al. (2010) for the sake of completeness. The model accounts for transmission blocking interventions in general, which may be as a result of natural infection that can be boosted with natural immunity or vaccines. In general, transmission-blocking interventions (TBIs) that directly target the parasite can be broadly classified as transmission-blocking vaccines (TBVs), discussed earlier, or transmission-blocking drugs (TBDs) (Delves et al., 2018; Wadi et al., 2018). As reported in Wadi et al. (2018), TBDs can be classified as follows: (i) **Drugs targeting the malaria parasite within the human-host**; This category includes: (*a*) drugs killing asexual stages of the parasite effectively and rapidly within human so that their progression to gametocytes may be stopped/reduced; (*b*) drugs reducing the commitment of asexual parasites to gametocytes within the human cycle, named as, the commitment blocking drugs; (*c*) drugs directly targeting immature and mature (stage $I-V$) gametocytes within the human; (*d*) drugs providing chemo-prophylaxis by directly acting on sporozoites, hence halting establishment of infection inside the human (Sinden, 2017; Wadi et al., 2018). (ii) **Drugs targeting the vector itself**, which includes a special class of drugs known as *endectocides* (Sinden, 2017; Wadi et al., 2018) (e.g. ivermectin), administered to humans that can kill a mosquito that draws blood from a human with the administered drug. Both (i) and (ii) are not the focus of this manuscript and would not be elaborated upon further. See Sinden (2017) and Wadi et al. (2018) for further details. (iii) **Drugs targeting the parasite in the vector**. This category comprises of antimalarial drugs that target the developmental stages (ingested gametocytes in the midgut of vector, male and female gametes, zygote, ookinete, oocyst and the sporozoites) of the parasite within mosquito vector (Sinden, 2017; Wadi et al., 2018) and fall within the scope of our work.

The rest of this paper is organized as follows. In Section 2, formulation of the mathematical model is presented. The basic mathematical results and their detailed proofs are illustrated in the Appendix. Numerical simulations and result are presented in Section 3 including the an estimate of the sporozoite density. A discussion of the results is presented in Section 4 and we conclude in section Section 5 giving ideas for future direction.

2. The mathematical model

Guided by the biology, the *Plasmodium falciparum* within-mosquito parasite forms are categorized at any time $t \geqslant 0$, into compartments described by the variables: G_{lM}, respectively, G_{lF}, representing the densities of the late stage male, respectively, female *Plasmodium falciparum* gametocytes picked by a female *Anopheles* mosquito from an infectious human after a successful blood meal; G_M, respectively, G_F, representing the densities of male, respectively, female gametes that arise via gametogenesis from the respective gametocytes of identical gender after the blood meal has settled within the mosquito midgut; Z, the density of zygotes formed as a result of fertilization between male and female gametes; T, the density of ookinetes produced from zygotes within the mosquito; O, the density of oocysts produced from ookinetes, and S, the density of salivary glands sporozoites, produced mature oocysts burst. A summary of the definitions of the state variables

and their quasi-dimension is shown on Table 1. Throughout, we adopt the following measurement notations: time is measured in *days*, volume in micro-litre, μL, density of late stage gametocytes are measured in number of gametocytes per unit volume, denoted by $gam/\mu L := \mathrm{G}$, densities of the developmental stages of the parasite within the mosquito (gametes, zygotes, ookinetes, oocysts, sporozoites) are measured by number of parasites per volume (density of parasites), denoted by $pa/\mu L := \mathrm{P}$ and density of human adaptive immune effectors within mosquito's midgut taken with blood measured in number of cells per unit volume denoted by $cells/\mu L := \mathrm{I}$. Throughout this study, densities refer to number per volume of blood. We now describe the derivation of the equations governing the time rate of change of each of the identified state variables. The assumptions used are governed by the within-mosquito biology and past work, see Aly et al. (2009), Baton and Ranford-Cartwright (2005), Teboh-Ewungkem and Yuster (2010), Woldegerima (2020). A conceptual schematic illustrating the flow dynamics of the within-mosquito developmental stages of the *P. falciparum* parasites is shown in Fig. 1.

(i) **Equation for male and female gametocytes:** When a female *Anopheles* mosquito bites an infected human, she may pick up the late stage (mature) gametocytes with the blood meal. If the blood meal contains both male (G_{lM} and female gametocytes G_{lF}) the within-mosquito vector dynamics can begin, upon successful insertion into the mosquito's gut. We assume that a mosquito picks an initial density of G_{l0} late stage gametocytes in a blood meal, which then decays exponentially thereafter. Of the ingested gametocytes, we assume that a fraction $\tilde{m}$ are male while the remaining fraction $1-\tilde{m}$ are female, so that the initial value of late stage male gametocytes ingested is $G_{lM}(0) = \tilde{m}G_{l0}$ and that of female gametocytes is $G_{lF}(0) = (1-\tilde{m})G_{l0}$, respectively, with $G_{lM}(0) + G_{lF}(0) = G_{l0}$. The differential equation quantifying the time rate of change of the densities of the male female gametocytes thereafter take the forms $\frac{dG_{lM}}{dt} = -c_1 G_{lM}, G_{lM}(0) = \tilde{m}G_{l0}$, and $\frac{dG_{lF}}{dt} = -d_1 G_{lF}, G_{lF}(0) = (1-\tilde{m})G_{l0}$, respectively, where c_1 is the rate at which male gametocytes exflagellate to produce male gametes while d_1 is the rate at which female gametocytes transform (emerge) to produce female gametes, both via gametogenesis. So, at any time $t \geqslant 0$, the respective densities of the male and female gametocytes in the mid gut of the mosquito are given by

$$G_{lM}(t) = \tilde{m}G_{l0}e^{-c_1 t},\ G_{lF}(t) = (1-\tilde{m})G_{l0}e^{-d_1 t}\ \forall t \geqslant 0, \tag{1}$$

Table 1
Description of state variables and their quasi-dimensions.

Variables	Description	Quasi-dimension
G_{lM}, G_{lF}	Density of late stage male (G_{lM}) and female (G_{lF}) gametocytes picked by a feeding mosquito after a successful blood meal that still remain as gametocytes at time $t \geqslant 0$.	G.
G_M, G_F	Densities of male (G_M) and female (G_F) gametes at time $t > 0$.	P
Z	Density of zygotes at time $t > 0$.	P
T	Density of ookinete at time $t > 0$.	P
O	Density of oocysts at time $t > 0$.	P
S	Density of salivary glands sporozoites at time $t > 0$.	P
E_a	Density of human adaptive immune effectors within mosquito's midgut taken with during a blood meal.	I

(ii) **Equation for the human antibodies:** We assume that the mosquito picks a density $\tilde{E}_{a0}$ of antibodies (part of the adaptive immune cells) with the blood meal, and once it is inside the mosquito's gut, it decreases as time increases at a rate $\tilde{\beta}$, where $\tilde{\beta}$ is the rate at which the blood meal is digested. Thus, we have that $\frac{dE_a}{dt} = -\tilde{\beta}E_a(t)$, with initial condition $E(0) = \tilde{E}_{a0}$, so that the density of antibodies (adaptive immune response) inside the mosquito's midgut is

$$E_a(t) = \tilde{E}_{a0}e^{-\tilde{\beta}t}, \forall t \geqslant 0. \tag{2}$$

(iii) **Equation for the densities of male and female gametes:** Within minutes of ingestion, the ingested gametocytes in a blood meal undergo **gametogenesis** (Aly et al., 2009; Baton and Ranford-Cartwright, 2005). The process starts and culminates with the female gametocytes producing v_1 female gametes (G_F) per female gametocytes within a 5 min after the blood meal, meanwhile the male gametocytes exflagellate producing $s_1 \geqslant v_1 \geqslant 1$ male gametes (G_M) per gametocyte about 10 min later (Baton and Ranford-Cartwright, 2005). Thus, male gametes emerge some 15 min after the blood meal. Hence, during the period of gametogenesis, the density of late stage male and female gametocytes decrease (see Baton and Ranford-Cartwright (2005)) and we assume the rates are c_1 and d_1, respectively. It is worth noting that compared to the female gamete produced, most of the male gametes produced are not viable (Baton and Ranford-Cartwright, 2005; Teboh-Ewungkem and Yuster, 2010; Teboh-Ewungkem et al., 2010). Let $\tilde{\alpha}_1$ be the fraction of the male gametes that are viable and $\tilde{\alpha}_2$ be the fraction of the female gametes that are viable, then the effective density of male gametes produced per male gametocytes is $s_1 c_1 \tilde{\alpha}_1$ while $v_1 d_1 \tilde{\alpha}_2$ is the effective density of female gametes produced per female gametocytes. Generated male and female gametes can die at rates a_1 and b_1, respectively, or before death, undergo the process of fertilization. During fertilization, male and female gametes fuse to form a zygote through gene mixing. According to the biological literature (Baton and Ranford-Cartwright, 2005), fertilization and fusion occur in a approximately 75 min after the blood meal (i.e. within 60 min after male gametes emerge and 70 after female gametes emerge) and we denote the fertilization rate by β_4. However, the process of fertilization can be inhibited by the human adaptive immune effectors picked up with the blood meal. We model this inhibition process by the factor $\frac{1}{1+\xi E_a}$, where ξ represents the efficiency of the inhibition process (Baton and Ranford-Cartwright, 2005; Bousema et al., 2011; McQueen et al., 2013). We note here that an effective antibody load/efficiency is considered to be when it results to the production of less than one oocyst.
Thus, the equations describing the densities of male (G_M) and female (G_F) gametes are, respectively, defined as:

$$\frac{dG_M}{dt} = s_1\tilde{\alpha}_1 c_1 G_{lM} - a_1 G_M - \frac{\beta_4 G_M G_F}{1+\xi E_a(t)},\ G_M(0) = 0 \tag{3}$$

and

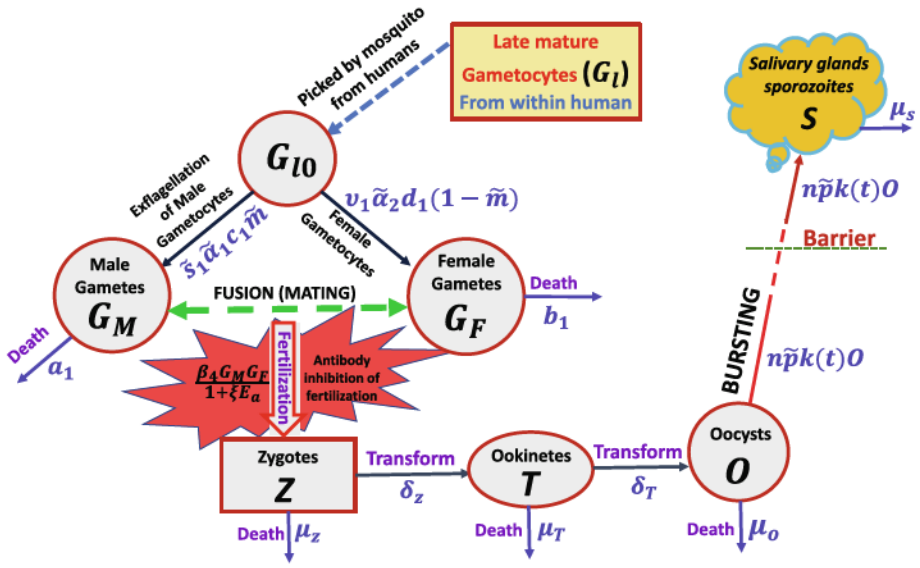

Fig. 1. Flow diagram for the within mosquito developmental stages of malaria parsites. A proportion of the late stage matured gametocytes (male and female) picked by Anopheles mosquito used as an input for the starting point of the within mosquito cycle. Male gametocytes exflagellate via gametogenesis producing male gametes. A fusion of male and female gametes which leads to a generation of zygotes. Zygotes transform to motile ookinetes. Ookinetes establish oocysts, and then mitosis begins. The sporoblast forms and sporozoites will be produced. Sporozoites travel to the salivary glad and are available for transfer to humans during the next blood meal. The descriptions of the parameters are given in Table 2.

$$\frac{dG_F}{dt} = v_1\tilde{\alpha}_2 d_1 G_{lF} - b_1 G_F - \frac{\beta_4 G_M G_F}{1+\xi E_a(t)},\ G_F(0) = 0. \tag{4}$$

(iv) **Equation for the density of zygotes:** The end product of a successful fertilization is the fusion of male and female gametes to form a zygote.
Zygotes can transform into motile ookinetes through the process of meiosis at rate δ_z, a process that takes between 10 and 30 h (Baton and Ranford-Cartwright, 2005; Teboh-Ewungkem and Yuster, 2010), or they can die naturally at a per capita rate μ_z. So, the equation governing the zygote population is

$$\frac{dZ}{dt} = \frac{\beta_4 G_M G_F}{1+\xi E_a(t)} - \mu_z Z - \delta_z Z,\ Z(0) = 0. \tag{5}$$

(v) **Equation for the density of ookinetes:** Mature ookinetes appear in approximately 20 h after a blood meal (Baton and Ranford-Cartwright, 2005; Vinetz, 2005). Those that successfully cross the peritrophic matrix after their migration through the blood meal enter the midgut epithelium where their transformation to oocysts commences. We denote the transformation rate of from ookinetes to oocycts by δ_T, and this process occurs approximately $24-48$ hours after the blood meal. The unsuccessful ookinetes die at a per capita death rate of μ_T. Hence, the equation for the density of the ookinete stage parasites is:

$$\frac{dT}{dt} = \delta_z Z - \mu_T T - \delta_T T,\ T(0) = 0. \tag{6}$$

(vi) **Equation for the density of oocysts:** Oocysts undergo extensive growth through mitosis and sporoblast formation, completes its development within 10–14 days (Aly et al., 2009) after the original blood meal, resulting in the production of thousands of sporozoites at a time dependent rate of $k(t)$. It is worth noting that other authors have reported 5–7 days (Baton and Ranford-Cartwright, 2005) and 6–9 days (Beier, 1998). Oocysts also die naturally at a per capita death rate of μ_o. It has been reported in Baton and Ranford-Cartwright (2005) and Beier (1998) that oocysts can survive the entire sporogony period. Thus, we the oocyst parasite population is modelled by

$$\frac{dO}{dt} = \delta_T T - \mu_o O - k(t)O,\ O(0) = 0. \tag{7}$$

(vii) **Equation for the density of sporozoite:** Sporozoites will be released from oocysts within $1-2$ weeks after a blood meal. Of these sporozoites produced per oocysts, only a fraction $\tilde{p}$ of them make it to the salivary glands. Sporozoites die naturally at a rate μ_s. Once the sporozoites have reached the mosquito's salivary glands, they can survive there for the remainder of the life of the mosquito (Baton and Ranford-Cartwright, 2005; Beier, 1998) unless they are injected by the mosquito to a vertebrate host during the next bite by the mosquito for a blood meal.
The transformation rate of oocysts to produce sporozoites is represented here by a function $k(t)$ for all $t \geqslant 0$. To determine the nature of $k(t)$, we must examine more closely the events that lead to the formation of the sporozoites from the mature oocysts many days after the initial ingestion of the infected blood meal by an *Anopheles* mosquito (Aly et al., 2009; Baton and Ranford-Cartwright, 2005; Beier, 1998). There is some variance in the timing as noted earlier: a range of 5–7 days was reported by Baton and Ranford-Cartwright (2005), 6–9 days by Beier (1998) and 10–14 days by Aly et al. (2009). Since the end of sporoblast formation is the precursor to the realization of sporozoites formation, we shall use roughly the midway point in these times to assume that sporozoites can become available in the salivary glands of the mosquito at about the 10th day (a choice used in Teboh-Ewungkem and Yuster (2010) and Teboh-Ewungkem et al. (2010)). We believe this is more reasonable also given how long a mosquito lives in the wild. Thus we

shall assume that, once an oocyst matures and sporoblast formation commences, there is a very fast change around the 10th day of development to produce sporozoites. So, we can estimate a range for the rate of conversion from mature oocyst to produce sporozoites, $k(t)$, as:

$$k(t) = \begin{cases} 0, & \text{if } \ 0 \leqslant t < 10 - \varepsilon^2, \\ \frac{\kappa}{2\varepsilon^2}(t - 10 + \varepsilon^2), & \text{if } \ 10 - \varepsilon^2 \leqslant t < 10 + \varepsilon^2, \\ \kappa, & \text{if } \ t \geqslant 10 + \varepsilon^2 \end{cases} \tag{8}$$

with $\kappa \in [\frac{1}{9}, \frac{1}{7}]$ (see Teboh-Ewungkem and Yuster (2010) and Teboh-Ewungkem et al. (2010)) and $0 < \varepsilon \ll 1$ is very small positive number showing that there is a rapid shift from almost no sporozoites to some amount of sporozoites at around $t = 10$ days. Hence, we write

$$\frac{dS}{dt} = n\tilde{p}k(t)O - \mu_s S, S(0) = 0, \tag{9}$$

where, n is En cas de doute, veuillez contacter notre assistance 24/7 UBA CFC: 01-2808822, cfc@ubagroup.com the number of sporozoites produced per bursting oocysts.

Therefore, all in one, the equations governing the developmental stage dynamics of malaria parasites within the mosquito is given by the non-linear system of ODEs:

$$\left.\begin{aligned} \tfrac{dG_{lM}}{dt} &= -c_1 G_{lM}, \quad G_{lM}(0) = \tilde{m}G_{l0}, \\ \tfrac{dG_{lF}}{dt} &= -d_1 G_{lF}, \quad G_{lF}(0) = (1-\tilde{m})G_{l0}, \\ \tfrac{dG_M}{dt} &= s_1\tilde{\alpha}_1 c_1 G_{lM} - a_1 G_M - \tfrac{\beta_4 G_M G_F}{1+\xi E_a(t)}, \ G_M(0) = 0, \\ \tfrac{dG_F}{dt} &= \nu_1\tilde{\alpha}_2 d_1 G_{lF} - b_1 G_F - \tfrac{\beta_4 G_M G_F}{1+\xi E_a(t)}, \ G_F(0) = 0, \\ \tfrac{dZ}{dt} &= \tfrac{\beta_4 G_M G_F}{1+\xi E_a(t)} - \mu_z Z - \delta_z Z, \ Z(0) = 0, \\ \tfrac{dT}{dt} &= \delta_z Z - \mu_T T - \delta_T T, \ T(0) = 0, \\ \tfrac{dO}{dt} &= \delta_T T - \mu_O O - k(t)O, \ O(0) = 0, \\ \tfrac{dS}{dt} &= n\tilde{p}k(t)O - \mu_s S, \ S(0) = 0, \\ \tfrac{dE_a}{dt} &= -\tilde{\beta}E_a(t), \ E(0) = \tilde{E}_{a0}, \end{aligned}\right\} \tag{10}$$

where, $E_a(t)$, the density of a human's adaptive immune response effectors within the mosquito's midgut at time t picked during a blood meal, is defined in Eq. (2). A summary of the parameters used in the model together with their descriptions and quasi-dimension is given in Table 2.

We note that the basic mathematical properties of system (10); positivity, boundedness and uniqueness of solutions, that ascertain that model solutions are mathematically and physically realizable are given in the Appendix. An analytic general solution, at least in integral form, also Appears in the Appendix.

3. Numerical simulations, results and sensitivity analysis

The solutions to system (10) are obtained via numerical integration using the parameter values given in Table 3 and initial conditions given in Table 4. The feasible parameters obtained, guided by the biological literature, were discussed in detail in Teboh-Ewungkem and Yuster (2010) and Teboh-Ewungkem et al. (2010). Additionally, two parameters of interests appearing in model (10) are estimated and their sensitivity discussed. These two parameter are $E_a(0)$, the size of ingested human antibodies within a blood meal, and ξ, a parameter that measures the efficiency of the ingested antibody's functionality. One would expect these parameters to vary depending on the mechanism by which the human antibodies were generated; whether naturally initiated as a result of the human being naturally exposed to the malaria parasite (Bousema et al., 2011; Ouédraogo et al., 2011), or whether it was drug or vaccine initiated (Blagborough et al., 2012). Moreover, it would also depend on the state of the human from whom the blood meal was taken, whether recently exposed or not (Ouédraogo et al., 2011). The literature on the specific mentioned parameters are not copious. However, using information from Saul (2008), we will allow the number of ingested human antibodies to vary from a small size to 100 in a blood meal and the efficiency ξ to vary from zero to unity, in order to quantify their individual and combined impacts on the size of the number of oocysts produced in an infected mosquito. In what follows, we consider the dynamics to be based on only a single blood meal taken by the feeding female anopheles mosquito. We understand that during their lifetime, mosquitoes feed on average every two to three days (see Ngwa et al., 2014; Ngwa et al., 2019; Teboh-Ewungkem et al., 2019), but we do not consider that here, except what happens when a single blood meal is taken. This is reasonable and informative and the results based on a single blood meal are easily extendable, when appropriate, to multiple blood meal feeding episodes if we consider the time lag between meals and the length of time it takes for mature oocysts to burst to release sporozoites (it takes about 10 days). That means oocysts that result from a second and hence subsequent blood meals would lag by about 2–3 days period for each additional blood meal, in their sporozoite production. One can then account for the total sporozoite load from two or more blood meals by summing up the sporozoites

Table 2
Description of parameters and their quasi- dimensional units. We measure time in *days*, and volume in μL.

Parameter	Description	Quasi-dimension
$\tilde{E}_{a0}$	Initial density of adaptive immune cells picked during blood meal.	I
G_{l0}	Initial density of gametocytes picked during blood meal.	G
$\tilde{\beta}$	Rate of decay of blood meal within mosquito gut.	$Time^{-1}$
$\tilde{m}$	Proportion of male gametocytes picked by the mosquito.	1
$1-\tilde{m}$	Proportion of female gametocytes picked by the mosquito.	1
c_1	Rate at which male gametocytes transform (exflagellate) to produce male gametes via gametogenesis.	$Time^{-1}$
d_1	Rate at which female gametocytes transform (emerge) to produce female gametes via gametogenesis.	$Time^{-1}$
s_1	Number of male gametes produced per male gametocytes	$P \times G^{-1}$
ν_1	Number of female gametes produced per female gametocytes	$P \times G^{-1}$
$\tilde{\alpha}_1$	Fraction of male gametes that are viable	1
$\tilde{\alpha}_2$	Fraction of female gametes that are viable	1
a_1	Death rate/failure rate of male gametes	$Time^{-1}$
b_1	Death rate/failure rate of female gametes	$Time^{-1}$
β_4	Fertilization rate of male and female gametes	$P^{-1} \times Time^{-1}$
ξ	Efficiency of adaptive immune effectors in inhibiting fertilization	I^{-1}
μ_z	Zygote death rate	$Time^{-1}$
δ_z	Zygote transformation rate to ookinetes	$Time^{-1}$
δ_T	Ookinetes transformation rate to oocysts	$Time^{-1}$
μ_T	Ookinetes death rate	$Time^{-1}$
μ_o	Mature Oocysts death rate	$Time^{-1}$
$k(t)$	Mature Oocysts bursting rate	$Time^{-1}$
n	Number of sporozoites produced per bursting oocysts	1
$\tilde{p}$	Fraction of sporozoites that make it to the salivary glands	1
μ_s	Natural death rate of sporozoites	$Time^{-1}$

Table 3
Within mosquito host dynamics: Range and baseline of parameter values and their quasi- dimensional units. In Teboh-Ewungkem and Yuster (2010), a detailed and elaborate description of the parameter ranges as well as the biological basis leading to the derivation of the ranges was presented. Thus, we do not repeat that here.

Parameter	Range of values	Baseline value	Quasi-dimension	Ref.
$\tilde{\beta}$	$[\frac{2}{3}, \frac{10}{2}]$	$\frac{10}{3}$	day^{-1}	estimated
$\tilde{E}_{a0}$	varies	11	$Cells/\mu L$	estimated
G_{I0}	$[10, 1000]$	300	$gam/\mu L$	Teboh-Ewungkem and Yuster (2010)
$\tilde{m}$	$(0, 0.5]$	0.25	1	Teboh-Ewungkem and Wang (2012) and Teboh-Ewungkem and Yuster (2010)
$1-\tilde{m}$	$(0.5, 1]$	0.75	1	Teboh-Ewungkem and Wang (2012) and Teboh-Ewungkem and Yuster (2010)
c_1	≈ 96	96	day^{-1}	Teboh-Ewungkem and Yuster (2010)
d_1	≈ 288	288	day^{-1}	Teboh-Ewungkem and Yuster (2010)
s_1	$[4, 8]$	8	$(para/\mu L) \times (gam/\mu L)^{-1}$	Teboh-Ewungkem and Yuster (2010)
v_1	1	1	$(para/\mu L) \times (gam/\mu L)^{-1}$	Teboh-Ewungkem and Yuster (2010)
$\tilde{\alpha}_1$	$(0, 4)$	0.39	1	Teboh-Ewungkem and Yuster (2010)
$\tilde{\alpha}_2$	$(0, 1]$	1	1	Teboh-Ewungkem and Yuster (2010)
a_1	$[\frac{1440}{25}, \frac{1440}{15}]$	$\frac{1440}{20}$	day^{-1}	Teboh-Ewungkem and Yuster (2010)
b_1	$[\frac{1440}{30}, \frac{1440}{20}]$	$\frac{1440}{25}$	day^{-1}	Teboh-Ewungkem and Yuster (2010)
β_4	$(0, 0.15]$	0.08	$(para/\mu L)^{-1} \times day^{-1}$	Teboh-Ewungkem and Yuster (2010)
ξ	$[0, 1]$	0, 0.8	$(Cells/\mu L)^{-1}$	Aikawa et al. (1981)
μ_z	1	1	day^{-1}	Teboh-Ewungkem and Yuster (2010)
δ_z	$[\frac{24}{23}, \frac{24}{19}]$	$\frac{24}{19}$	day^{-1}	Teboh-Ewungkem and Yuster (2010)
μ_T	$[1, 1.5]$	1.4	day^{-1}	Teboh-Ewungkem and Yuster (2010)
δ_T	$[0.5, 1]$	0.6	day^{-1}	Teboh-Ewungkem and Yuster (2010)
μ_o	0	0	day^{-1}	Teboh-Ewungkem and Yuster (2010)
$k(t)$	See Eq. (8)	See Eq. (8)	day^{-1}	Teboh-Ewungkem and Yuster (2010)
κ	$[\frac{1}{9}, \frac{1}{7}]$	$\frac{1}{8}$	day^{-1}	Teboh-Ewungkem and Yuster (2010)
ε^2	$[10^{-12}, 10^{-4}]$	10^{-5}	day	estimated
n	$[1000, 10000]$	3000	1	Teboh-Ewungkem and Yuster (2010)
$\tilde{p}$	$[0.1, 0.25]$	0.2	1	Teboh-Ewungkem and Yuster (2010)
μ_s	$[\frac{1}{6}, \frac{1}{4}]$	$\frac{1}{6}$	day^{-1}	estimated

Table 4
Initial Conditions at time $t = 0$ for model (10) (Teboh-Ewungkem and Yuster, 2010).

State variable	E_a	G_{IM}	G_{IF}	G_M	G_F	Z	T	O	S
Initial Value	$\tilde{E}_{a0}$	$\tilde{m}G_{I0}$	$(1-\tilde{m})G_{I0}$	0	0	0	0	0	0

from the first, second and subsequent blood meals. Again, this assumption does not account for those mosquitoes that do not succeed in getting a full blood meal and live to seek again within a short time.

3.1. The role of human antibodies in inhibiting fertilization of gametes and sporozoite load

3.1.1. No antibody influence on within-mosquito fertilization and sporozoite load

We begin this section with the numerical simulations when no antibody effects inhibit fertilization of male and female gametes within a mosquito, i.e. the term $\xi E_a(0) = 0$. Now, $\xi E_a(0) = 0$ if either (i) $E_a(0) = 0$, that is no antibodies are ingested initially with the blood meal, or (ii) $\xi = 0$, that is the ingested antibodies' functionality in inhibiting fertilization and impacting parasite development within the mosquito is negligible. Another possibility is that both ξ and $E_a(0)$ are small so that their combined effect is negligible. The case $E_a(0) = 0$ can be thought of as a scenario in which a blood meal was taken by a female anopheles mosquito from an infected individual who was not recently exposed since per the results in Ouédraogo et al. (2011) it was suggested that naturally acquired immunity against two of the antigens that begin their expression in intracellular gametocyte within naturally exposed human hosts, Pfs48/45 and Pfs230, was a function of recent exposure rather than of cumulative exposure to gametocytes. In the same article no age dependency. This can manifest itself in areas of very low malaria transmission (hypoendemic regions) whereby due to the low transmission, the inhabitants are less exposed to infective mosquito bites when compared to a high transmission area where the inhabitants are more prone to infective mosquito bites. Thus, inhabitants in higher transmission regions have a higher propensity to have recent infections, even though the infec-

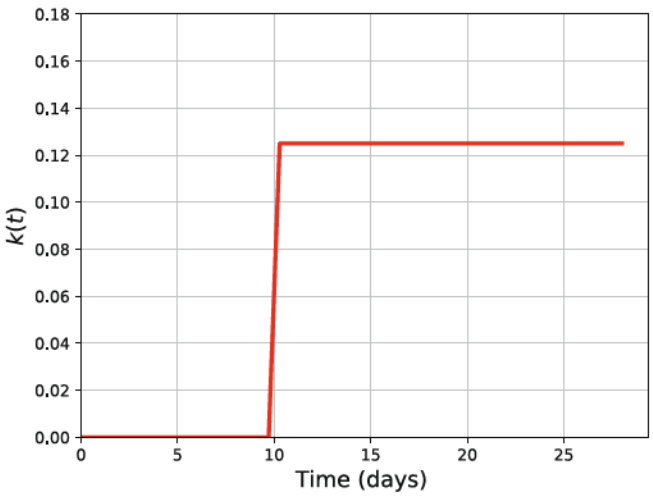

Fig. 2. Plot of the time-dependent production rate function of sporozoites from mature oocysts, plotted for $\varepsilon = 1 \times 10^{-5}, \kappa = \frac{1}{8}$ as t runs from 0 to 28 days.

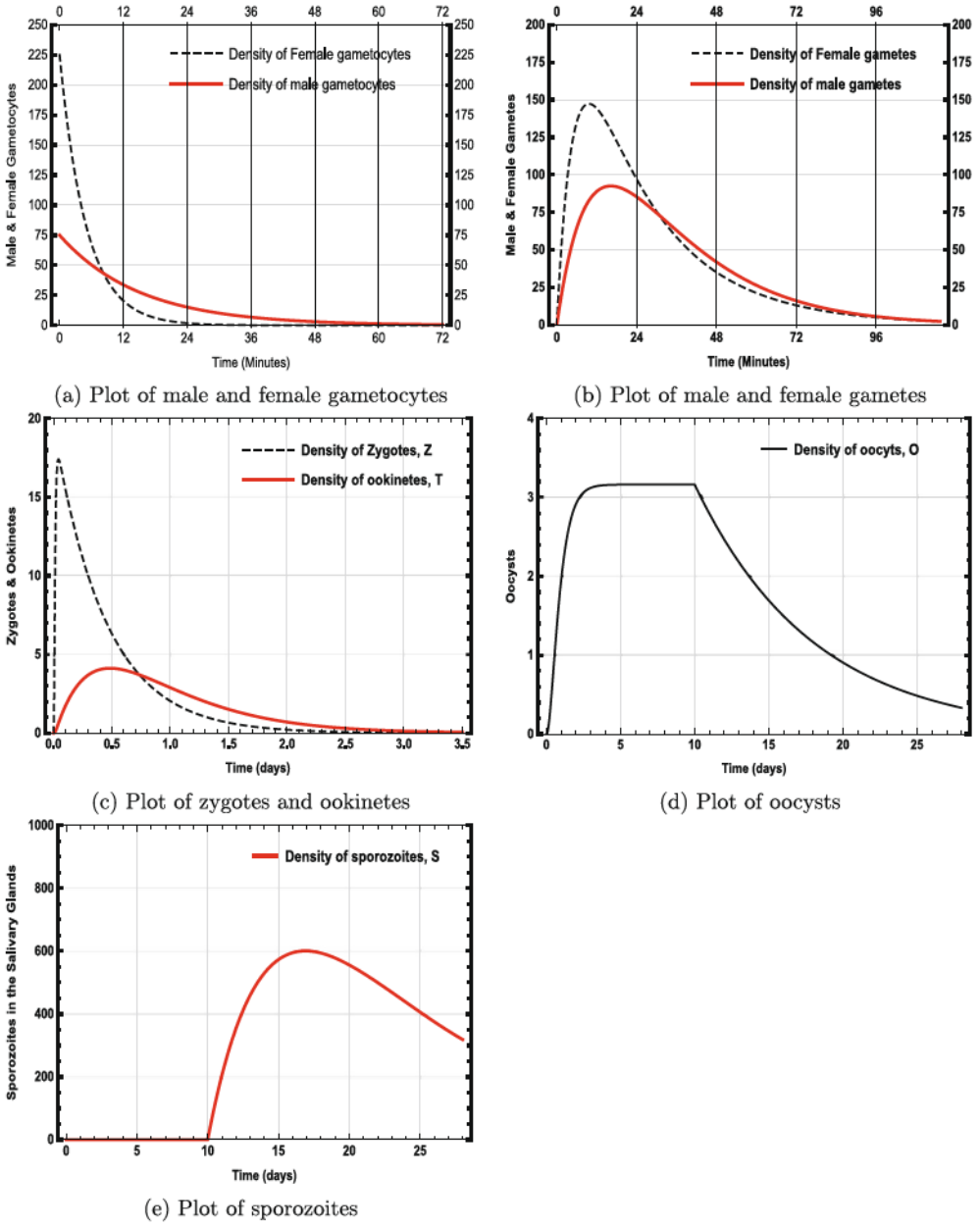

(a) Plot of male and female gametocytes

(b) Plot of male and female gametes

(c) Plot of zygotes and ookinetes

(d) Plot of oocysts

(e) Plot of sporozoites

Fig. 3. Trajectory solutions of model system (10) in the case when $\xi = 0$ so that human antibodies/adaptive immune effectors have no effect on fertilization and zygote development of malaria parasites within the mosquito.

tions may not be severe for adults and children with a better defined adaptive immune response (see Hay et al., 2008; Manore et al., 2019; Teboh-Ewungkem et al., 2014; Teboh-Ewungkem et al., 2015 for more on naive and mature immune individuals and disease severity). On the other hand, the case $\xi = 0$ can represent a scenario in which the ingested antibodies are not at full functional performance level and this could be corrected with boosting of the naturally acquired sexual stage specific antibody response with boosting either via a TBD or TBV. In the absence of experimental measurements, a combined effect in which the product $\xi E_a(0) = 0$ might be more meaningful. Solution curves for the scenario in which $\xi E_a(0) = 0$ are shown in Fig. 2,3. This basically reproduces Fig. 3 of Teboh-Ewungkem and Yuster (2010).

Fig. 3a shows solution curves of the densities of late stage gametocytes in the mosquito midgut after a blood meal, plotted for 0.05 days, that is, approximately 72minutes, a time frame that captures roughly the life span of gametocytes. The trajectories show that the densities of both male and female gametocytes decaying to zero within the plotted time. Fig. 3b shows trajectories of densities of male and female gametes plotted in 0.08 days (about 1.9 h) which shows the female and male gamete population sizes increasing from zero to some bounds (as gametogenesis occurs) reaching their peaks slightly beyond 5 and 15 min, respectively, and then reducing back to zero. By the end of the last process, fertilization between male and female gametes occur producing zygotes. Zygotes density increases from zero to reach an upper bound. The produced zygotes undergo meiosis to form ookinetes, the later, the progeny of oocysts. Both zygotes and ookinetes drop to an average of less than by 1 each by day 2. Their solution profiles are plotted in Fig. 3bc. Fig. 3bd and e show trajectories for the densities of oocysts and sporozoites, respectively plotted for a time period of 28 days which is taken to represent the lifespan of a feeding female mosquito. Oocysts reach a maximum density in approximately 2 days after a blood meal, a time within which mature oocysts are considered to have been established and made entrance into the midgut epithelium (Baton and Ranford-

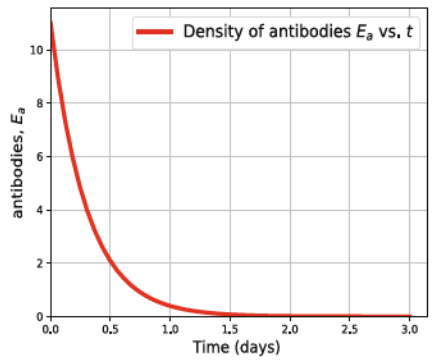

(a) Density of antibodies in the mosquito, $E_a(t)$ vs. time

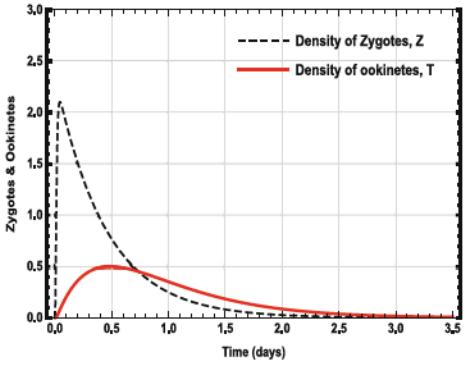

(b) Plot of zygotes

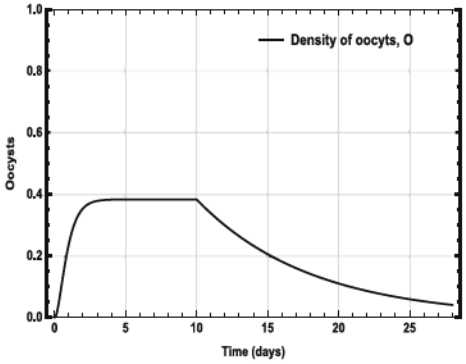

(c) Plot of oocysts

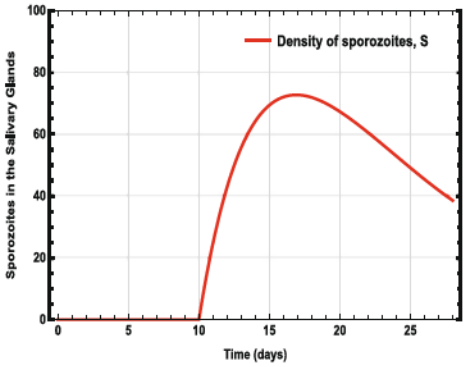

(d) Plot of sporozoites

Fig. 4. Solution curves of model system (10) in the case when $\xi = 80\%$.

Cartwright, 2005; Teboh-Ewungkem and Yuster, 2010). Mitosis begins with sporoblast formation happening, and at about the 10th day, sporozoites are released from bursting oocysts (see Fig. 3d and e). Sporozoites stay in the salivary glands until the next mosquito bite or the mosquito dies.

3.1.2. Antibody influence on within-mosquito fertilization and sporozoite load

In this subsection, we consider the role of ingested antibodies and their potential impact on fertilization of male and female gametes, and hence, subsequent within parasite development. The profile for the ingested immune effectors are exponentially decaying functions, decaying from $E_a(0) = 11$ (taken as the initial condition and baseline value) immune cells in an ingested blood, as shown in Fig. 4a, where blood meal sizes range from 2 to 10 μL (Gaston Pichon et al., 2000; Teboh-Ewungkem and Yuster, 2010). When these antibodies/adaptive immune response play a role we consider the dimensionless term $\xi E_a(0) = 8.8 \neq 0$, where $\xi = 0.8$ can be thought of as the efficiency with which the ingested immune factors function and $E_a(0) = 11$ is the ingested number of antibodies. See Figs. 4d for the solution curves for the zygote, ookinete and oocyst populations, as well as the resulting sporozoite load, when antibody effects are considered. The choice of $\xi = 0.8$ was based on an electron microscopical study in Aikawa et al. (1981) and also a study in Rener et al. (1980). We remark that the studies were on *Plasmodium gallinaceum* and not *Plasmodium falciparum*, the parasite under study in this manuscript. However, it gives us a starting point, especially with limited information. Comparing Figs. 3 and 4, it is easy to see that the densities of zygotes, ookinetes, oocysts and the sporozoite load all reduce significantly in the presence of antibodies. Specifically, the maximum average zygote density of about 17.5 in the absence of antibodies (Fig. 3c), reduces to approximately and average of 2.1 (Fig. 4b) when the effects of antibodies are considered. Likewise, the ookinete peak reduces from about 4 (see Fig. 3c) with no antibody effect to approximately 0.5 (Fig. 4b) with antibodies assumed to function at 80% efficiency, an 87.5% drop. Similar effects can be seen in the oocyst densities (comparing Figs. 3d and 4c), with maximum peak of slightly above 5 reducing to under 1, which in turn would yield fewer sporozoite load. The corresponding sporozoite peak densities are approximately 600 (Fig. 3e) with no antibody effect, dropping to approximately 70 (Fig. 4d) with antibody effects. These drops in the sporozoite load do not only occur at the peaks and endpoints, they occur at each time frame from the 10th day until the mosquito dies. These illustrated decreases in the peak densities of the within-mosquito parasite forms correlate with decreases in total population sizes of these forms. We note that compared to the model in Teboh-Ewungkem and Yuster (2010), the sporozoite peak density when no antibody effect is considered is slightly lower in this manuscript (see Fig. 3e) compared to the corresponding sporozoite maximum density in Fig. 3d of Teboh-Ewungkem and Yuster (2010), which was at 1500 mainly because of the death term considered in this model. We next compute the cumulative sporozoite sum.

3.1.3. Estimation of the cumulative sum of sporozoite density

The end result of the within-mosquito processes after a blood meal from an infectious human is the production of sporozoites, the form of the parasite transmissible from mosquitoes to humans. Thus, it is desirable to estimate the cumulative sum of sporozoite density (or running total density), which we denote by S_{cumsum}. We will also compute the total, S_{area}, and average S_{avg}, sporozoite densities produced at the end of the within-mosquito process,

based on a single blood meal. The effective average, which is the average over the time after oocysts release sporozoites would also be computed. We start with the computations of the total and average densities and compare the results for the case when no human antibody effects are in action, that is $\xi E_{a0} = 0$, and in when human antibody effects function to inhibit and slow fertilization. For the latter case, $\xi = 80\%$ and $E_{a0} = 11$ immune cells per ingested blood meal, so that $\xi E_{a0} = 8.8 \neq 0$. The estimate of the total sporozoite density produced, which is the area under the graph of the solution curves for $S(t)$ between the lines $t = 0$ and $t = t_{end} = 28$ days (see Figs. 3e and 4d), and that of the average densities are computed via the respective functions,

$$S_{area} = S_{cumsum}(t_{end}) = \int_0^{t_{end}} S(t)dt \text{ and } S_{avg} = \frac{1}{t_{end} - 0} \int_0^{t_{end}} S(t)dt.$$

These definite integrals are then estimated using the composite Simpson's rule in Python, were a step size of $h = 0.56$ was chosen, leading to the partitioning of the time interval $[0, 28]$ days into $n = 50$ sub intervals. For the case with no human effectors in effect, the cumulative sum is $S_{area} = \int_0^{28} S(t)dt = 14,663.38$ sporozoites, yielding an average sporozoites density of $S_{avg} = \frac{1}{28-0} \int_0^{28} S(t)dt = 523.69$ and an effective average density of $\frac{1}{28-10} \int_{10}^{28} S(t)dt = 814.63$. On the other hand, in the case of antibody effect, we obtain the total $S_{area} = 1775.83$ so that $S_{avg} = 63.42$ with the effective average value of 98.66 sporozoites.

Next, we compute the cumulative sum of the sporozoite density up to time t, as the load increases during the considered time frame. This cumulative sum is a sequence of partial sums computed by partitioning time using a uniform step size and then numerically extracting the densities of sporozoite (the sequences) from the solution curves 3e and 4d at the endpoints of the partitioned time. We then use the function "*cumsum*" from the library "*numpy*" in Python to plot the total sum of the extracted data up to time t. Plots of the cumulative sum of the sporozoite densities showing their increase with time are shown in Fig. 5. At the end of the process for the considered time frame (28 days), the total cumulative sporozoite density in the salivary gland of the feeding mosquito is $S_{area} = S_{cumsum}(28) = 24,500.88$ sporozoites for the case where $\xi E_{a0} = 0$ (no antibody effect) and $S_{area} = S_{cumsum}(28) = 3921.83$ sporozoites for the case where $\xi E_{a0} \neq 0$, a much smaller sum when antibody effects are considered. In all, the cumulative sum of sporozoite density when $\xi E_{a0} \neq 0$, is much lower than that in the absence of the action of antibodies in inhibiting fertilization.

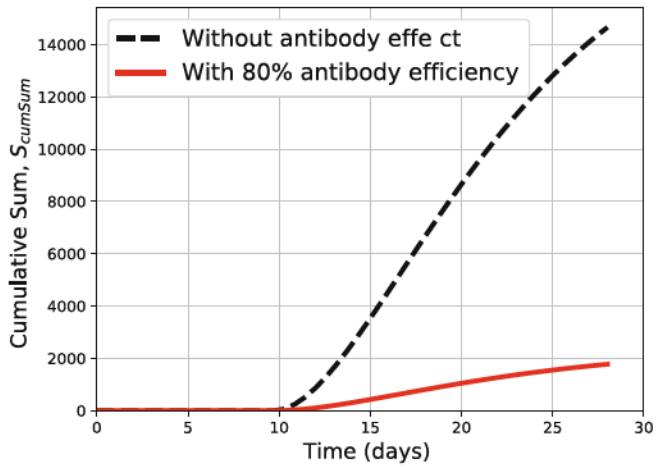

Fig. 5. Plots of cumulative sums of sporozoite densities produced for model system (10) without any effect of human-antibodies, i.e. $\xi E_{a0} = 0$, and for the case with human-antibody effects, where $\xi = 80\%, E_{a0} = 11$ initial immune cells picked up in a blood meal so that $\xi E_{a0} = 8.8$.

3.2. Comparative and sensitivity analyses of individual parameters and their combined effects on the model solution outcomes

Here, we investigate how individual parameters as well as a combination of parameters influence the model solution, an outcome. The parameters to be considered are the immune-related parameters ξ and $E_a(0)$, the initial number of ingested gametocytes G_{I0} and the fertilization rate β_4. Similar analyses for G_{I0} and β_4 were carried out in Teboh-Ewungkem and Yuster (2010) in the absence of antibody effects, where it was shown that when all other parameters were held fixed with a gametocyte sex ratio of 0.25 used (i) higher sporozoite load corresponded to high numbers of ingested gametocytes and the relationship was more than linear; and (ii) higher sporozoite load corresponded to higher fertilization rate, although in this case, the relationship was less than linear. Moreover, the combined effects of both G_{I0} and β_4 illustrated that control schemes that targeted both parameters yielded a stronger positive impact. In particular, if $G_{I0} < 100$ regardless of how high β_4 was or if $(G_{I0}, \beta_4) \in [0, 200] \times [0, 0.04]$, then a more desirable outcome in which less that one oocyst was produced was observed. We now seek to replicate that study under immune effects and begin by looking at the impacts of the individual variables.

3.2.1. Sensitivity analysis of the individual impacts of the immune-related parameters: ξ and $E_a(0)$

In this subsection, we investigate the effects of the immune-related parameters, ξ and $E_a(0)$, in reducing the different parasite densities in the mosquitoes, with oocyst density and hence sporozoite load key outputs, as well as the sensitivities of these outputs to changes in the individual parameters. By sensitivity, we refer to the degree at which an input parameter influences the model output, with sensitive parameters those which have a significant influence on the model outcomes (Hamby, 1994). These analysis can help inform strategies aimed at controlling infectious diseases (Woldegerima et al., 2018; Wu et al., 2013), and in our scenario the within-host parasite infection in the mosquito.

Fig. 6 shows the oocyst densities and sporozoite loads as we vary the efficiency rate, ξ for values in the set $\{0\%, 20\%, 40\%, 60\%, 80\%, 100\%\}$. The figure shows that as we increase ξ, the oocyst densities and hence sporozoite loads both decrease. Thus oocyst density and sporozoite loads are negatively correlated to human antibodies and thus the sensitivity index on oocyst density and sporozoite load is negative. Moreover, it is easily seen that increasing ξ from 0 to 0.2 (20% increase), the peak oocyst is reduced by more than 60%.

Next, in Fig. 7, we vary the initial size of the ingested human antibodies, $E_a(0)$, that can picked up in a blood meal, while maintaining the efficiency ξ and all other parameters fixed at the baseline values in Table 3 with the initial data as given in Table 11. Values of $E_a(0)$ are selected from the set $\{0, 5, 11, 25\}$. As illustrated in Fig. 7, the dynamics is similar to the case of increasing ξ, whereby an increased number of ingested immune cells correlates with a decrease in oocyst density and sporozoite load. What is strongly evident is that a high number of immune cells need to be picked up to see a strong and desirable response with possibly the production of less than 1 oocyst that can mature.

3.2.2. Sensitivity analysis of the individual impacts of the number of ingested gametocytes and fertilization rates under immune effects: G_0 and β_4

Here, we investigate the sensitivity of the oocyst density to changes in both the size of the number of ingested gametocytes and the fertilization rate, when human under immune factors are

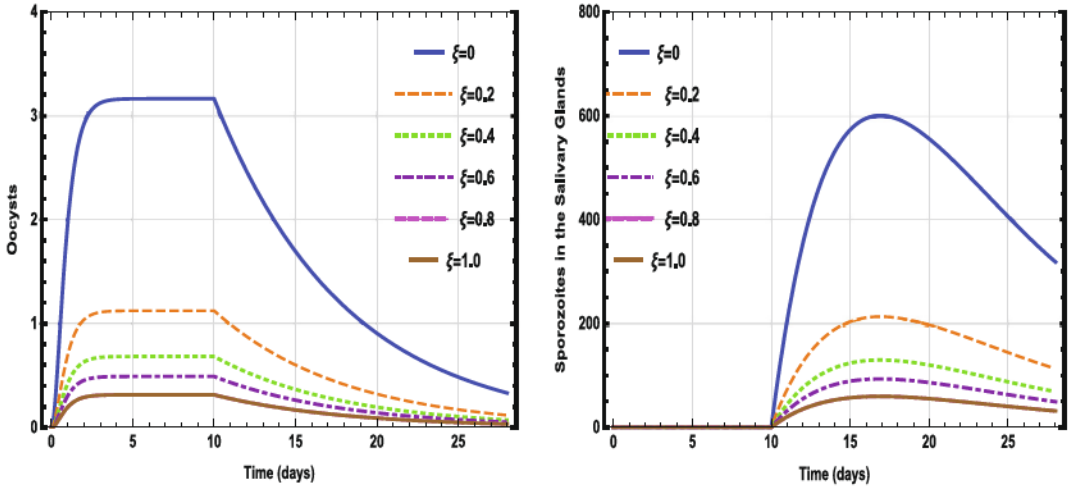

(a) Sensitivity of oocysts load to ξ (b) sensitivity of sporozoites load to ξ

Fig. 6. Plots of sensitivities of the response outputs for the number of oocysts and sporozoites as we vary ξ, choosing ξ values from the set $\{0\%, 20\%, 40\%, 60\%, 80\%, 100\%\}$, while maintaining the other parameters fixed as in Table 3. The figures show that antibodies have a positive impact in reducing oocyst density and sporozoite load. Notice that beyond 60% efficiency in antibody function, the reduction effect is not as drastic when compared with the effects at values of ξ higher than 60%.

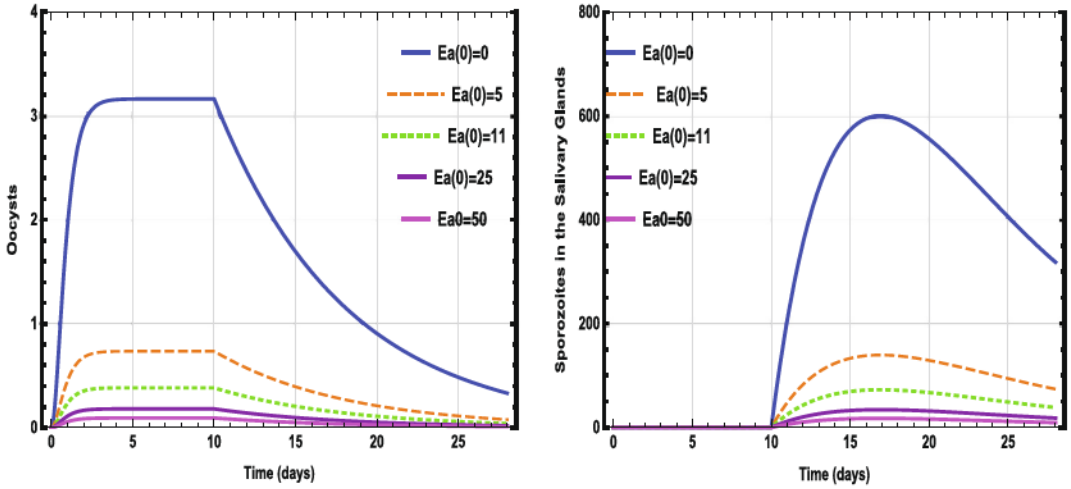

(a) Oocysts for different values $E_a(0)$ (b) Sporozoites for different values $E_a(0)$

Fig. 7. Sensitivity of solution curves of system (10) to changes in the initial values of the amount of human antibodies, $E_a(0)$, that can be ingested in a blood meal with all other parameters maintained at base values. as in Table 3. The initial values for the other state variables are held fixed as in Table 11. We vary $E_a(0)$ by using values in the set $\{0, 5, 11, 25\}$. We see that the higher the number of ingested human immune effectors the smaller the oocyst load and sporozoite density.

in effect. We vary G_{l0} by selecting values from the set $\{100, 300, 600, 800, 1000\}$, a biological feasible range as described in Teboh-Ewungkem and Yuster (2010). With $\tilde{m} = 0.25$, which is the proportion of gametocytes that are males so that $1 - \tilde{m} = 0.75$ are females. Thus, for the stated G_{l0}, we have $mG_{l0} \in \{25, 75, 100, 150, 200, 250\}$, and the plots are shown in Fig. 8. The result when no immune effectors were in effect was discussed in Teboh-Ewungkem and Yuster (2010), where it was shown that the parameter which had the greatest impact in sporozoite load reduction, under the stated conditions here, was the initial number of gametocytes. In particular, even at a high fertilization rate, the number of ingested gametocytes had a stronger influence on oocyst density, whereby for any $G_0 < 100$, the number of generated oocyst was less than 1. Now, with antibody effects at the base levels chosen such that $\xi E_a(0) = 8.8$, we see that at higher levels of ingested initial gametocytes with a blood meal, the we can still achieve the desirable less than one oocyst, see Fig. 8. That is, the antibody effects enhances the control such that a blood meal taken from an immune mature humans in which the immune parameters are at the base levels as in Table 3, is less infectious than one of same size taken from a naive immune human. By less infectious, here we mean a blood meal that results in less than one oocyst production such that sporozoite production cannot occur.

In Fig. 8, we look at how sensitive the solution curves of system (10) are to changes in the number of ingested gametocytes, G_{l0}, that can be picked with the blood meal, while in Fig. 9, we look at sensitivities with respect to the fertilization rate between male and female gametes, β_4, that can be picked with the blood meal. In Fig. 8, we simulate the codes for values of $G_{l0} \in \{100, 300, 600, 800, 1000\}$ with the initial values defined by Eq. (11) for each chosen G_{l0}, while all parameters are set at the base parameters as defined in Table 3. The plots show that as we increase G_{l0}, the oocyst density and sporozoite load increase.

Similarly, in Fig. 9, the model is simulated for values of $\beta_4 \in \{0.02, 0.04, 0.06, 0.08, 0.1, 0.12, 0.14\}$ with all parameters are set at the base parameters as defined in Table 3. The plots show

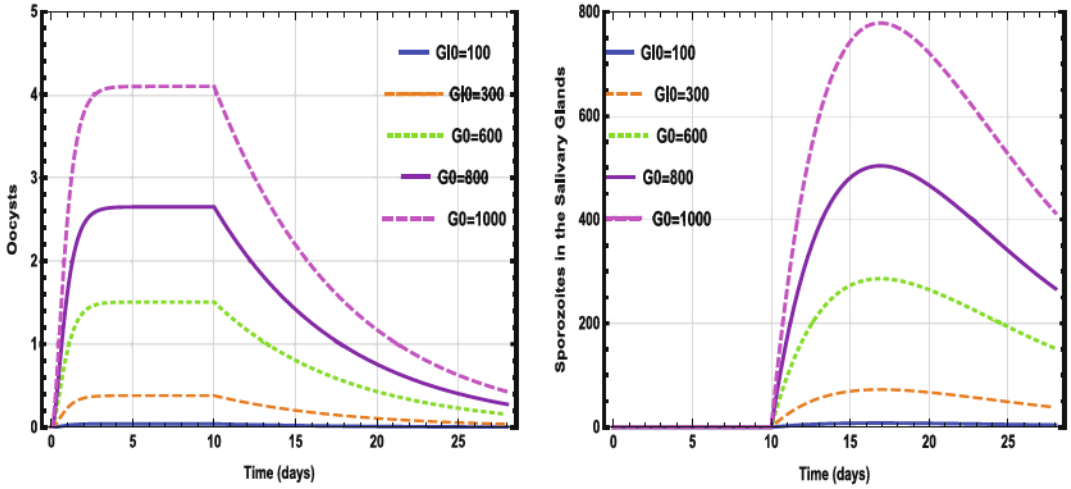

Fig. 8. Solution trajectories showing the sensitivity of the model output (solution) to changes in G_{I0}, where G_{I0} varies through the values in the set $\{100, 300, 600, 800, 1000\}$. The plots show that as we increase G_{I0}, the oocyst density and sporozoite load increase.

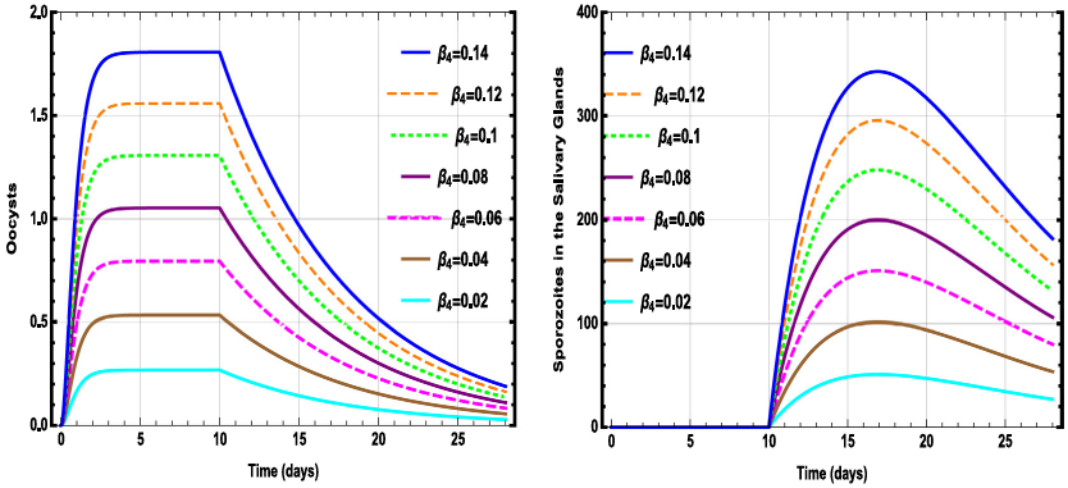

Fig. 9. Solution trajectories showing the sensitivity of the model output (solution) to changes in β_4, where β_4 varies through the values in the set $\{0.02, 0.04, 0.06, 0.08, 0.1, 0.14\}$. Likewise, as β_4 increases the oocyst density and sporozoite load both increase.

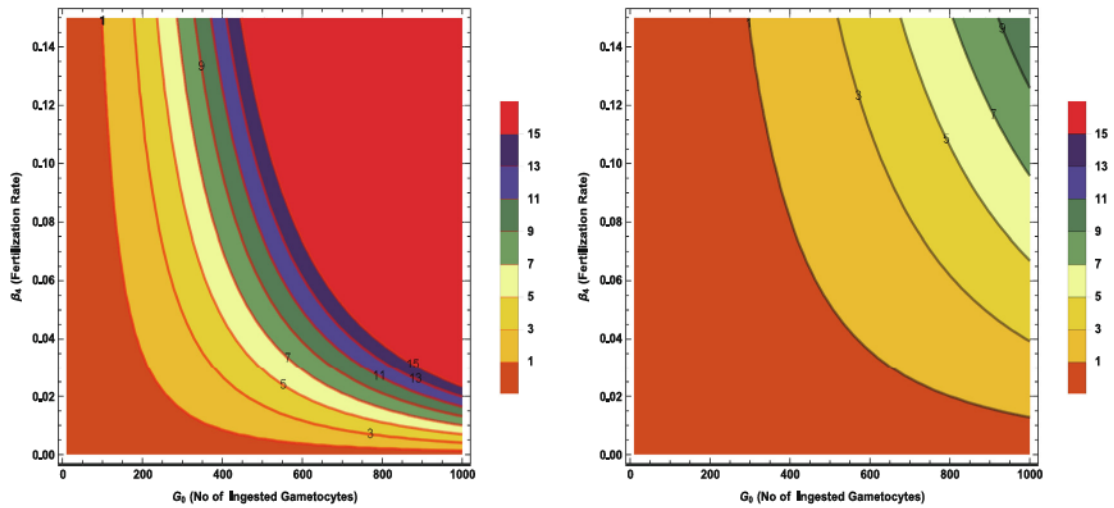

(a) When $\xi E_{a0} = 0$, i.e. no immune effects. (b) When we fix $\xi = 0.8$ and $E_{a0} = 11$.

Fig. 10. Contour plot showing the average number of oocysts for different male and female gamete fertilization rates, β_4, and number of gametocytes, G_0, ingested with a blood meal. In Fig. 10a, there are no immune effects, meanwhile in Fig. 10b, we consider the baseline immune effects with all other parameters kept fixed as in Table 3.

similar increases in oocyst density and sporozoite load with increase in β_4.

3.2.3. Sensitivity analysis of the combined impacts of fertilization rate and the number of ingested gametocytes under immune effects: G_0 and β_4

We begin by looking at the contour plots for oocyst density as both fertilization rate, β_4, and the number of ingested gametocytes, G_{l0}, are varied. See Fig. 10. Clearly, for any fixed G_{l0}, as fertilization rate increases the oocyst load increases. This is true regardless of immune effects. However, the immune effects is quite evident as the region in the (G_{l0}, β_4) space for which a density of less than 1 oocyst is produced on average is much larger, depicted by the brown region. If a larger percentage of gametocytes are ingested together with acquired immune effects taken to be the base value, then even with slightly higher fertilization rate, it is possible that the mosquito may not successfully become infectious, despite being infected. Our focus is on the oocyst density because it is more informative, as one oocyst on average implies the mosquito can be considered infectious as that one oocyst can produce 1000 to 10,000 sporozoites upon bursting, after about 10 days. Thus, a control scheme aimed at reducing the size of G_{l0} and augmenting immune effectors picked up with reducing fertilization potential is quite desirable. This is even more important because the first two named strategies are strategies that can occur within the human. In particular, an infected human that seeks to complete their antimalarial treatment using non-fake drugs in a timely manner can help to reduce the gametocytes within the said human and hence reduce the potential for high number of gametocytes that can be picked up by a blood feeding mosquito on humans. Additionally, the use of a potential transmission blocking drug or vaccine administered to a human can help boost the humans' sexual-staged immune status and hence the size of ingested immune effectors, which can help diminish the fertilization potential of male and female gametes generated from the corresponding male and female gametocytes.

3.2.4. Sensitivity analysis of the combined impacts of fertilization rate and immune-related parameters: β_4, ξ and/or $E_a(0)$.

Here, we seek to understand the extent of the impact on oocyst density as we vary a pair of the model parameters from among β_4,

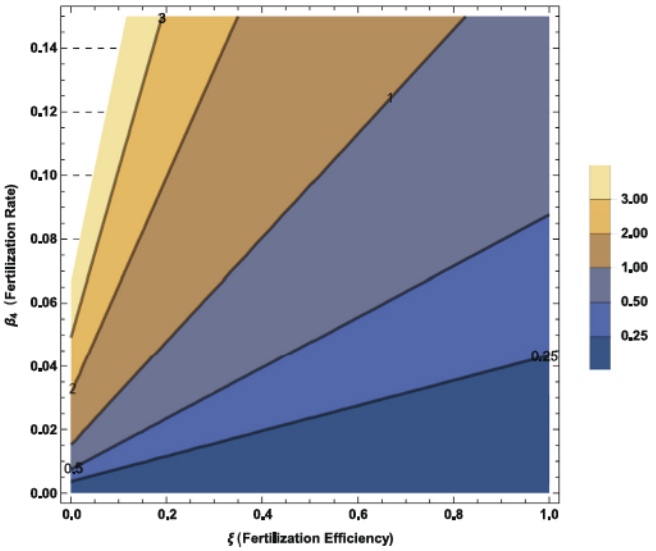

Fig. 11. Contour plot of the average density of oocysts as fertilization rate, β_4, and the efficiency of human-antibodies, ξ, are varied, for a fixed size of initial ingested gametocytes $E_a(0) = 11$. The remaining parameter values are fixed to at the baseline values as in Table 3.

the fertilization rate, ξ the immune efficiency and E_{a0}, the initial number of ingested human antibodies. We begin with β_4 versus ξ, their combined effect on oocyst density while E_{a0} is held fixed at a size of 11 immune Cells per blood meal (see Fig. 11). As we vary both, we clearly see that even at the highest fertilization rate of $\beta_4 = 0.14$, an efficiency of 0.8 can render the biting mosquito eventually non-infectious with an average of less than one oocyst produced. Thus a control strategy that reduces both β_4 versus ξ, is desirable.

A similar result is obtained when we vary β_4 versus E_{a0}. In particular, we look at β_4 versus E_{a0}, their combined effects on oocyst density, while holding ξ fixed at two values 0.5 and 0.8 as shown in Fig. 12. Comparing Fig. 12a and b, we see similar results that shows the regions in the (E_{a0}, β_4) space for which we have less than one average oocyst is larger for $\xi = 0.8$ (Fig. 12b) than for $\xi = 0.5$ (Fig. 12a). For $\xi = 0.8$ we can achieve less than 1 average oocyst even at the highest fertilization rate considered. Moreover, the control effort required for this latter case is less than the control effort for $\xi = 0.5$.

A more important comparative study, especially as it relates to transmission blocking drugs and/or vaccines, seems to be one that looks at oocyst load as a function of fertilization rate β_4 and $\xi E_a(0)$, which gives the cumulative impact of antibodies in inhibiting fertilization of male and female gametes. The contour plots of the oocyst density is shown in Fig. 13. The combined effect of $\xi E_a(0)$ is now convoluted in that a small $\xi E_a(0)$ value might mean that.

(i) $E_a(0)$ is small and $\xi$is small so that $\xi E_a(0)$ is small;
(ii) ξ is small, closer to zero but $E_a(0)$ is not as large such that ξE_a is small, i.e. even though the initial density of $E_a(t)$ is large, the combined impact of $\xi E_a(0)$ is insignificant in reducing production of oocysts;
(iii) $E_a(0)$ is small and $\xi$is large, can be close to 1, but the fact $E_a(0)$ is small diminishes the combined effect of the product $\xi E_a(0)$ so that it is small.

From Fig. 13a, it is quite clear that for the cases when fertilization rate is quite high, the desirable impact of a small oocyst density (with a desirable density of less than one oocyst) can only potentially be achieved when $\xi E_a(0)$ is very large, say larger that 8. This is, if either ξ is close to one and $E_a(0)$ is much larger than 8 or ξ is small but $E_a(0)$ is much larger such that $\xi E_a(0)$ is larger than 8. Clearly at a fertilization rate of $\beta_4 = 0.8$ the $(\xi, E_a(0))$ region is depicted in Fig. 13b illustrated by the regions above the purple. This is for the case when the initial ingested gametocytes are maintained at base values. If we now look at the oocyst densities as we vary the dimensionless immune effect ξE_{a0} against the size of the initial numbers of ingested gametocytes, we see that when with fertilization rate β_4 is fixed at base value of 0.08 (Fig. 14a), the range of G_{l0} varies that can be ingested for which we can have a less than one average oocyst is not that large. In fact, the desirable region with a less than one oocyst average increases but the increases is less than linear. A 50% reduction in fertilization rate to $\beta_4 = 0.04$ (Fig. 14b) provides a better results and larger region, but again the change is less than linear.

4. Discussion of results

The work here is an extension of the work in Teboh-Ewungkem and Yuster (2010), used to study through a mathematical model, the within mosquito-host life cycle of *Plasmodium falciparum* parasites under human immune effects. The model, a deterministic model, accounts for the developmental stage transformations of the within-mosquito dynamics of the malaria parasites from ingested gametocytes to sporozoites formation and seeks to illuminate the potential role of human antibodies that can be picked by a

feeding mosquito during blood meal in inhibiting or slowing down the development of the parasite within the mosquito. The late stage (mature) gametocytes picked from the human were used as an input into the mosquito and initiated the within mosquito dynamics part the dynamics. The proposed model was mathematically shown to be well-posed in the sense that solutions exists, remain non-negative, are bounded and can be uniquely determined for a given parameter set. We numerically compared the simulations results for the cases when $E_{a0}\xi = 0$ (i.e. either and $E_{a0} = 0$ or $\xi = 0$ or both are very small, hence no antibody effects) to the case when $\xi E_{a0} \neq 0$ (there is a human immune factor that can inhibit fertilization in the mosquito). In the latter case, $E_a(t)$ decays exponentially with time from its initial value $\widetilde{E}_{a0}$, at the same rate as the rate at which the ingested human blood-meal disintegrates. Our results indicate that an sexual stage immunity response that elicits an efficient functional transmission blocking activity in the human can lower oocyst density and hence sporozoite load in a mosquito (see Figs. 3 and 4).

Figs. 3 and 4 also illustrate that there is an overall dampening effect on the final outcome of the parasite development processes within the mosquito with immune factors considered. That is, increase in the size and efficiency of the antibodies in inhibiting fertilization leads to a decrease in the average oocyst density resulting in a lower sporozoite total load. We computed the cumulative sum of sporozoite density under the action of antibodies in inhibiting fertilization and compared it with the case when that was not so. With antibody effect, the cumulative sum was much lower (see Fig. 5). Both cumulative sums computed at end of 28 days yielded results that are within experimentally reported ranges, $1 \times 10^2 - 1 \times 10^5$, as noted in Baton and Ranford-Cartwright (2005) and Beier (1998). Thus, TBI is a plausible way of blocking transmission; suppressing the development of sporozoites within a mosquito, which will in turn reduce the number in an infected mosquito that would be available for transmission to humans during a blood meal by the infected mosquito. These results highlight the fact that ongoing research on transmission blocking interventions (TBI) can potentially be quite promising. If control measures can be developed which incorporates factors within the human that could enhance the action of antibodies to disrupt the fertilization process and hence within-mosquito parasite development, there could be great gains in reducing transmission from mosquitoes to the humans. We note that these human immune factors must function efficiently in disrupting/inhibiting fertilization so that the end product is an average oocyst density that is less than one. A successful production of just one oocyst that eventually bursts to release sporozoite does not inhibit nor reduce the transmissibility potential of sporozoites from mosquitoes to humans since one oocyst can produce 1000 to 10,000 sporozoites (Baton and Ranford-Cartwright, 2005; Teboh-Ewungkem and Yuster, 2010), which is undesirable if we intend to inhibit transmission from mosquitoes to humans.

Our numerical results highlight the fact that in understanding infectivity to mosquito, the key factors at play are the immune status of the individual from whom a blood meal is taken, the number of gametocytes ingested in a blood mean and hence the size of a blood meal, and the fertilization rate between male and female gametes that emerge via gametogenesis. Starting with gametocytes ingested, in Bousema et al. (2007) and the associated references therein, it was noted that both the presence of mature gametocytes in the peripheral bloodstream and the human host immunity were determinant factors for a successful transmission of *P. falciparum* from a human to a osquito. In a later field study conducted in three African countries by same author and collaborators (Bousema et al., 2011), it was shown that there was a positive correlation between mosquito gametocyte density and mosquito infection rates. On the other hand, in Rodriguez-Barraquer et al. (2018), it was shown that blood stage forms of malaria parasites decrease with age of individuals due to acquired immune effects against asexual stage parasites that develop with increases exposure to malaria. However, how the size of the asexual parasite forms correlate to gametocyte load and thus age, is not quite clear in general. For example in a cross sectional study in Ouédraogo et al. (2010), the authors showed that even though detection of gametocytes was more common in the children population, the percentage of asexual parasites that may then commit to develop into gametocytes may actually increase with age, which may weaken the correlation between high asexual forms and gametocyte load in both children and adults. The aforementioned highlight the complexity of malaria, a fact that is compounded by the known variability and heterogeneity that exists in parameters from field and laboratory studies, in addition to external influences, transmission settings and uncertainties around true parameter values. We believe our study thus play a significant role in that it can quantify the oocyst density regardless of the individual variations that exists. In particular, our results thus illuminates what outcomes can be observed under different scenarios of the studied parameter regime and under a wide parameter range as illustrated for fertilization rates, β_4, and initial ingested gametocyte size G_{I0}. For example in Fig. 10 compared to Fig. 10a and b), we illustrated that we can have outcomes where a mosquito is potentially infected, regardless of the individual from which a blood meal is taken as long as a combination of parameters within feasible parameter ranges results in the said outcome. That is a blood meal from two separate individuals may yield different sizes of ingested gametocytes as well as different fertilization rates, but produce same oocysts density in a mosquito.

Next the immune response of the individual, which in this case refers to the sexual-staged immune response that can elicit transmission blocking activity in the mosquito that fed from the individual is important. In particular, a blood-meal that results in a small $E_a(0)$ value or a small $\xi E_a(0)$ value would not be desirable if high numbers of gametocytes are ingested with the blood meal. In this case, the potential for that blood meal to render the mosquito infectious would be dependent upon the number of gametocytes ingested and the fertilization rate between male and female gametes (see Figs. 10 and 13a). A blood meal that results in the baseline values of the sexual-staged immune effects would contribute to serve as some sort of a control, hence reducing the region in (G_{I0}, β_4) space over which the feeding mosquito can produce an average of about 1 or more oocysts (see Fig. 10b).

We note that in some studies, like the one in Malawi by the authors in Churcher et al. (2016), it was shown that the highest odds of having gametocytes when infected was among school aged children (5–15 years), when compared to adults ($\geqslant$ 16 years) and under 5 years old children, who did not have a significant higher odds. Thus is it is clear that the inter-relationship between a human's adaptive immune status (which is a function of age), the gametocyte load and the immune effectors against gametocytes ingested from an individual, is a more complex problem and may depend on the malaria region, whether the region under study is a high transmission region or low transmission region or whether malaria is all year round and stable (holoendemic) or whether it is seasonal as well as the blood type of the individuals (de Jong et al., 2020). In a study in Bousema et al. (2007) involving Tanzanian adults in an area were malaria transmission is seasonal but high, the authors noted that the adults under study had a lower exposure to gametocytes when they were compared to the children population. However, the authors asserted that the antibody specific to the sexual staged parasites would then be expected to decrease with age, rather than increase. With our results that illustrate that due to these antibody effects, humans with little sexual-

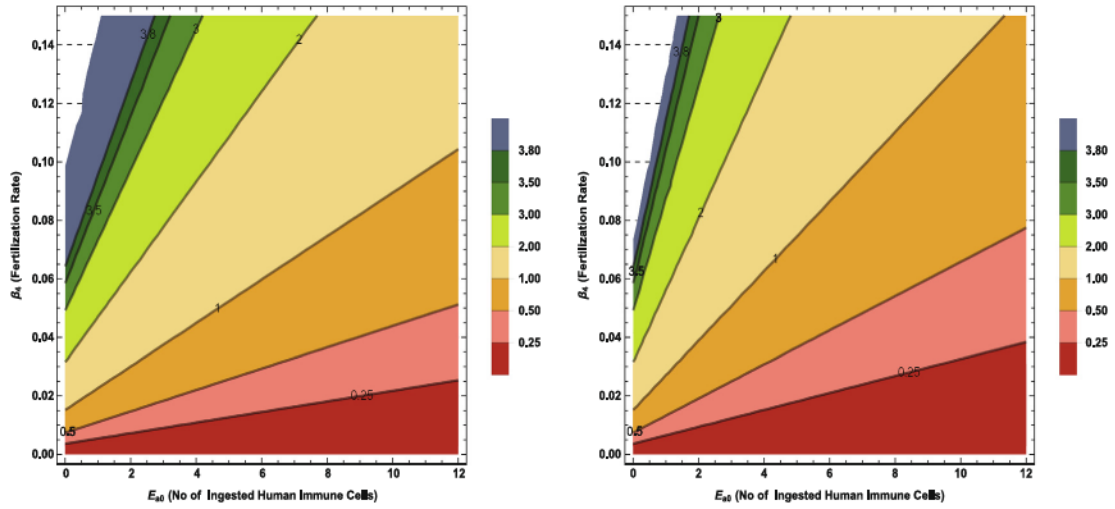

(a) When $\xi = 0.5$ fixed (b) When $\xi = 0.8$ fixed

Fig. 12. Contour plot of the average oocyst density as fertilization rate, β_4, and the initial number of ingested human-antibodies, $E_a(0)$, are varied for $(E_{a0}, \beta_4) \in [0, 12] \times [0, 1.5]$, with ξ fixed, wherer $\xi = 0.5$ is shown in Fig. 12a and $\xi = 0.8$ is shown in Fig. 12b. The remaining parameters are as given in Table 3.

staged immune response could be better mosquito infectors compared to those with sexual staged immune responses that can elicit a strong transmission blocking activity in the mosquito, the adult population who typically are the asymptomatic population may be a stronger reservoir of infection for malaria in many endemic regions, suggesting that they may be better mosquito infectors overall. However, we understand that these results may be more complex and one has to factor in the gametocyte load that is ingested in a blood meal, which we have also shown to be a determinant of the density of oocysts produced but also the quality of the gametocytes ingested, especially under adaptive immune pressure, how fecund they may be. We believe that our results presented here in the form of contour plots that show variable parameter spaces under which a mosquito could be infective is innovative and can be useful and applicable in a wide variety of malaria settings.

In some sense, understanding the combined effect of ξE_{a0} in reducing oocysts load seems more meaningful than studying each term individually. We did so in this manuscript. Some questions worth exploring then are: Does age increase the functional efficiency of these immune factors in inhibiting male and female gamete fertilization or not? In Bousema et al. (2007), where the authors showed that the adults under study had a lower exposure to gametocytes when compared to the children population but asserted that their sexual stage specific antibody would be expected to decrease with age, rather than increase, compels us to ask: How does such a potential decrease compare with the functional efficiency of the resulting antibody size? Or, in general, how does size versus functional efficiency complement each other? Figs. 13 and 14 show the relationships of oocysts load to these key parameters and hence how they can impact mosquito infectivity for different fertilization rates and gametocyte loads. What is strongly evident is that a high number of immune cells need to be picked up to see a strong and desirable response with possibly the production of less than 1 oocyst that can mature. It is worth noting that this parameter is hard to characterize fully. However

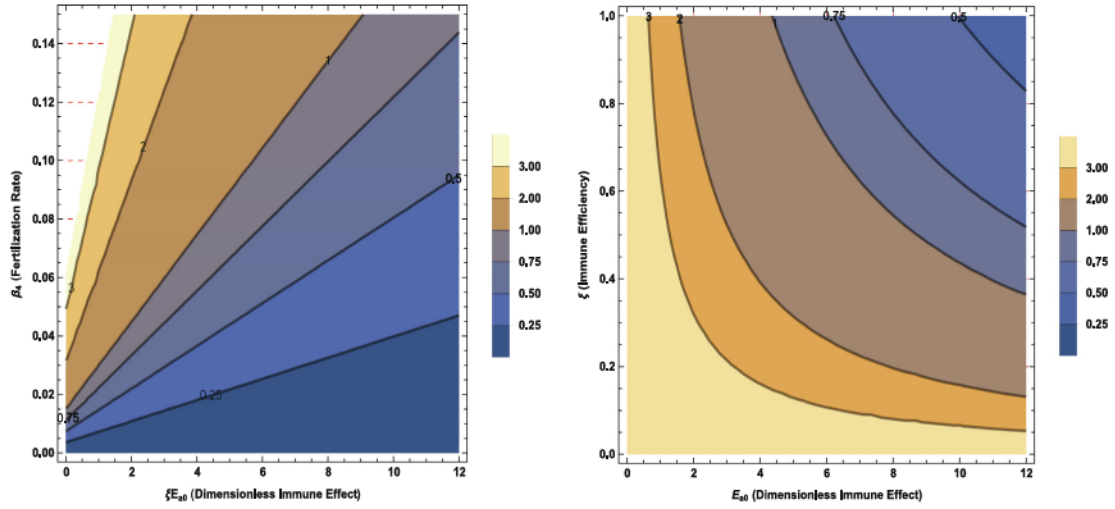

(a) β_4 versus the dimensionless immune effect ξE_{a0}. (b) ξ versus E_{a0} with β_4 held fixed.

Fig. 13. Contour plots of the average oocyst density as (i) fertilization rate, β_4, and the dimensionless immune effect ξE_{a0} are varied (Fig. 13a) and (ii) as ξ and E_{a0} are varied with $\beta_4 = 0.8$, held fixed (Fig. 13b). The remaining parameter values are as given in Table 3.

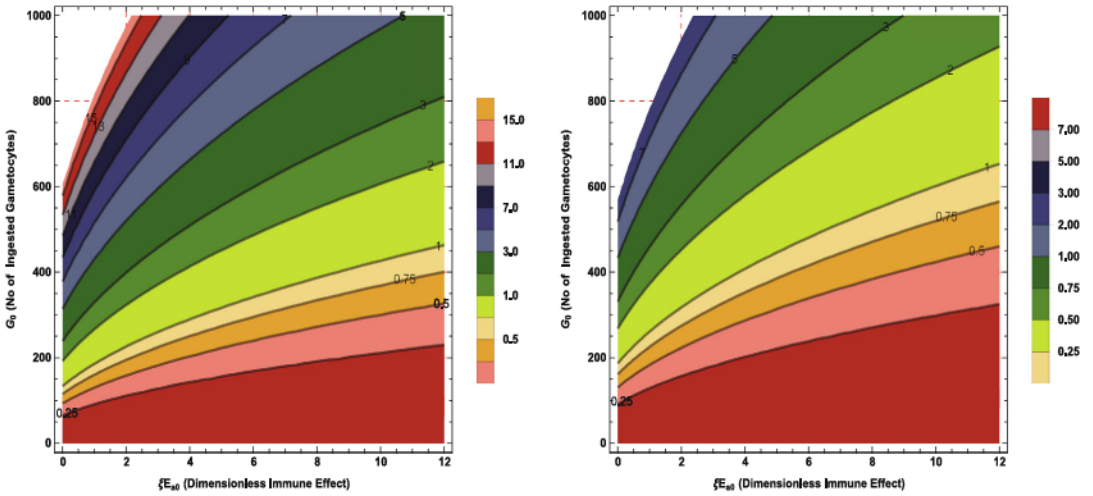

(a) β_4 versus the dimensionless immune effect ξE_{a0} with $\beta_4 = 0.08$.

(b) ξ versus E_{a0} with β_4 reduced by 50% to $\beta_4 = 0.04$.

Fig. 14. Contour plots of the average oocyst density as the dimensionless immune effect ξE_{a0} is varied against the size of the initial numbers of ingested gametocytes with fertilization rate β_4 is fixed at 0.08 (Fig. 14a) and then reduced by 50% to 0.04 (Fig. 14b). The remaining parameter values are as given in Table 3.

it leads to questions that experimentalists and biologists can explore, which are (1) how many immune cells and types can be picked up by a feeding mosquito during a blood meal? (2) Does the size of the immune effectors depend on the human from which the blood meal is drawn? (3) Can the efficiency of the ingested immune cells be quantified? If so, how? And these responses may differ in different transmission settings.

We believe that the work here can be beneficial to researchers developing further investigation so that its outcomes can help towards the current effort of developing transmission-blocking-vaccines (TBV) and/or transmission-blocking-drugs (TBD). The efficacy of transmission blocking interventions are usually measured as either a reduction of the prevalence of infected mosquitoes in field studies, or the reduction of oocyst density following membrane feeding assays (considered to be gold standard) in laboratory studies (Churcher et al., 2017; Churcher et al., 2012; Da et al., 2015; Wang et al., 2018). Our results that mathematically show sensitivities to oocysts density to variations in densities of ingested gametocytes, fertilization rate and immune effectiveness itself show the roles these variables play as important determinants that should be accounted for when discussing efficacy of transmission blocking intervention (TBI). Our model results can help to inform the determinants of membrane feeding studies to assess the efficacy of transmission blocking intervention in that we can quantity the number of oocysts produced after the intervention using antibodies. With laboratory data for the different developmental stages of the parasite within the mosquito fitted to our model, more specific predictions on the efficacy of such transmission blocking intervention (TBI) strategies could be inferred. In particular, in our work we showed using contour plots, how oocyst densities are affected for varied values of ingested gametocytes, fertilization efficiency and immune effects. The results are directly tied to reduction in oocysts density but can implicitly provide information on the prevalence of infected mosquitoes. For example, in Figs. 8 and 9, we showed how a reduction in ingested numbers of gametocytes in a blood meal is correlated to a reduction in oocyst load in one mosquito, when we assume an efficacy of $\xi = 0.8$ and $E_a = 11$. Likewise, when we fix the size of the ingested gametocytes and allow these immune effects to vary within each mosquito, higher efficiency and higher ingested immune factors was linked to lower oocyst density (see Figs. 11–14) in each mosquito. However, if we consider that different mosquitoes can ingest different densities of gametocytes in a blood meal, otherwise identical in all other respects, then we can infer that prevalence will be higher if more of the mosquitoes ingest higher densities of gametocytes. However, this is more complex as one would have to consider the fertilization effects within each of these mosquitoes. As illustrated in Fig. 11(a) and (b), fertilization rate impacts oocyst density in a mosquito, where by a reduction in oocyst density is observed even when high densities of gametocytes are ingested, as long as fertilization rate is low. Thus although prevalence seems to be linked to oocyst density, our results support the assertion that in general, transmission reducing interventions should report reduction of infected intensity and prevalence. Additionally, one has to be cautious as to what this might mean for possible infection to humans. In Churcher et al. (2017), it was shown that mosquito parasite load had a per bite influence on the probability of mosquito-to-human transmission, with malaria infection to vaccinated humans highly probable when the feeding mosquito had > 1000 residual-sporozoites in its salivary glands. In addition to oocysts intensity, sporozoite load are important output functions.

5. Conclusions

Malaria control strategies that focus on the use of insecticide treated bednets (ITNS), effective antimalarial drugs and control of mosquito populations are yielding some success in the field towards malaria control. However, even with the observed gains, malaria deaths are still high and the number of cases are still high. Additionally, compliance with regards to using and sleeping under ITNs as well anti-malarial drug resistance spread and insecticide resistance continue to complicate and make control challenging. Thus, development of effective malaria control strategies that can utilize human factors, such as the human immune effectors developed during within-human parasitemia, that would work to inhibit parasite development progress within the mosquito that fed from that human, continue to be desirable. Additional factors such as transmission blocking vaccines or transmission blocking drugs are also desirable and are also under investigation (Biswas, 2017; Carter, 2001; WHO, 2017). These methods aim to exploit the human-parasite-mosquito-human interaction as well as the fact that humans can be given these vaccines and/or drugs to target the parasite within the mosquito, hence disrupting the parasite

life-cycle and potentially disrupting successful transmission between humans and mosquitoes. Our results demonstrates that efforts geared towards this form of malaria control methodology, aimed at disrupting the malaria parasite life cycle in a mosquito can produce promising and desirable results. Moreover, if combined with the other malaria control methodologies, then a significant reduction in the morbidity and mortality or malaria among the hardest hit regions could be achieved, with malaria eradication a possibility.

The true nature and mechanism of the function of the human antibodies within the mosquito gut as well as the transition time and rate from sporoblast formation to presence of sporozoites in the salivary glands of the mosquito system remain to be investigated. It is also not clear to us if a mosquito can harbour different strains of the parasite in different stages of development or if there is selective development once a mosquito is infected. These are important questions that can affect the nature of the growth processes modeled in this manuscript.

Our model is a deterministic model, where the threshold of one oocyst production is defined as an effective transmission blocking activity. However, a further adaptation of the model could include a stochastic formulation in which we use probabilistic analysis to define the threshold parameter, whereby transmission blocking efficacy is defined as the probability that a mosquito is infected with oocyst versus not infected. This would be pursued in future studies. Furthermore, a comprehensive study that starts from the within human parasite levels to the mosquito parasite levels can help illuminate how human factors under a varied conditions can impact oocyst density and sporozoite load and hence disease prevalence.

CRediT authorship contribution statement

Miranda I. Teboh-Ewungkem: Conceptualization, Investigation, Supervision, Validation, Funding acquisition, Writing - review & editing. **Woldegebriel A. Woldegerima:** Conceptualization, Formal analysis, Methodology, Software, Visualization, Writing - original draft, Writing - review & editing. **Gideon A. Ngwa:** Formal analysis, Investigation, Supervision, Validation, Writing - review & editing.

Declaration of Competing Interest

The authors declare that they have no known competing financial interests or personal relationships that could have appeared to influence the work reported in this paper.

Acknowledgments

WA Woldegerima acknowledge the support from the DST/NRF SARChI Chair in Mathematical Models and Methods in Biosciences and Bioengineering at the University of Pretoria, Grant No. 82770, and National Science Centre of Poland, grant 2017/25/B/ST1/00051. MIT-E acknowledges the support of Lehigh University and GAN acknowledges the grants and support of the University of Buea, Cameroon and the Hochschule Mittweida University of Applied Sciences, Germany. GAN also acknowledges the Cameroonian Ministry of Higher Education through the initiative for the modernization of research in Cameroon's Higher Education. All authors also acknowledge the sponsorship of the Commission for Developing Countries (CDC) in conjunction with the International Mathematics Union (IMU) through the CDC-ADMP (African Diaspora Mathematicians Program) grant that made it possible for interactive collaborative work that lead to some of the work. MIT-E also acknowledges support via NSF grant 1815912 which enabled her engagement in completing the project.

Appendix A. Mathematical analysis of the developed model

Here we state and prove the basic mathematical properties of system (10). But, we start with the following remarks.

Remark 1. The functions $E_a(t)$ defined in 2, $G_{lM}(t)$ and $G_{lF}(t)$ defined in 1 are nonnegatiive, bounded and decreasing with time with the property that $0 < E_a(t) \leqslant \tilde{E}_{a0}$, $0 < G_{lM}(t) \leqslant \tilde{m}G_{l0}$, $0 < G_{lF}(t) \leqslant (1-\tilde{m})G_{l0}$ $\forall t \geqslant 0$ with $\lim_{t\to+\infty}(E_a(t), G_{lM}(t), G_{lF}(t)) = (0,0,0)$.

Remark 2. The function $k:[0,\infty)\to[0,\infty)$ given by (8) is nonnegative, bounded and continuous function of time with

$$0 \leqslant k(t) \leqslant \kappa,\ \forall t \geqslant 0,\ \text{and}\ \lim_{t\to(10-\varepsilon^2)^-} k(t) = \lim_{t\to(10-\varepsilon^2)^+} k(t) = 0 = k(0),$$
$$\lim_{t\to(10+\varepsilon^2)^-} k(t) = \lim_{t\to(10+\varepsilon^2)^+} k(t) = \kappa = k(10+\varepsilon^2).$$

Its plot with time is shown in Fig. 2. Additionally, it is continuous modification of the step-function rate used in Teboh-Ewungkem and Yuster, 2010; Teboh-Ewungkem et al., 2010.

Now, lets begin by defining $\boldsymbol{x} = (E_a, G_{lM}, G_{lF}, G_M, G_F, Z, T, O, S)^{Tr}$, (here Tr stands for transpose), to be a column vector in $\mathbb{R}^9$. Then, the initial conditions of system (10) can be written as:

$$\begin{aligned}\boldsymbol{x}(0) &= (E_a, G_{lM}, G_{lF}, G_M, G_F, Z, T, S)(0)\\ &= \left(\tilde{E_{a0}}, \tilde{m}G_{l0}, (1-\tilde{m})G_{l0}, 0, 0, 0, 0, 0\right),\end{aligned} \tag{11}$$

where, $\tilde{E_{a0}} \geqslant 0$ and $G_{l0} \geqslant 0$ are respectively the initial numbers per volume of ingested human adaptive immune cells and late stage gametocytes picked by mosquito during a blood meal from a vertebrate host. Next, lets define the biologically-feasible region $\mathscr{D}_v \subseteq \mathbb{R}^9_+$:

$$\mathscr{D}_v = \left\{ \begin{array}{l} (E_a, G_{lM}, G_{lF}, G_M, G_F, Z, T, O, S) \in \mathbb{R}^9 : E_a \geqslant 0, G_{lM} \\ \geqslant 0, G_{lF} \geqslant 0, G_M \geqslant 0, \\ G_F \geqslant 0, Z \geqslant 0, T \geqslant 0, O \geqslant 0, S \geqslant 0 \end{array} \right\}.$$

Then, we can rewrite our dynamical system (10) as an initial value problem (IVP) in the form

$$\boldsymbol{x}' = \Phi(\boldsymbol{x}),\ \boldsymbol{x}(0) = \boldsymbol{x}_0, \tag{12}$$

where, $\boldsymbol{x}:[0,\infty)\longrightarrow\mathbb{R}^9$ is a column vector of state variables as defined, and $\Phi:\mathbb{R}^9\times[0,\infty)\longrightarrow\mathbb{R}^9$ with $\Phi(\boldsymbol{x}) = (\phi_1,\cdots,\phi_9)^{Tr}(\boldsymbol{x})$ the vector valued function containing the right hand side of the system as it's components, and

$$\boldsymbol{x}_0 = (E_a(0), G_{lM}(0), G_{1F}, G_M(0), G_F(0), Z(0), T(0), O(0), S(0))^{Tr}$$

be the column vector containing the initial conditions of the system. Then we have the following theorems.

Theorem 1 (*Positivity and positive invariance of solution*). *Consider system (10) with initial conditions (11). If the initial data is in $\mathbb{R}^9_+$, then every solution of system (10) remains in $\mathbb{R}^9_+$. If additionally, the initial data satisfies $\boldsymbol{x}(0) = \boldsymbol{0}$, then the solutions of system (10) will remain zero for all $t > 0$. Thus, with respect to the system, $\mathbb{R}^9_+$ is positively invariant and attracting. Additionally, the system has a forward positive solution in $\mathbb{R}^9_+$, once it starts there.*

Proof of Theorem 1 (Positivity and positive invariance of solution):

First, if $\boldsymbol{x}(0) = \mathbf{0} = (0,0,0,0,0,0,0,0,0)$, then using Eq. (12), $\boldsymbol{x}'(0) = \Phi(\mathbf{0}) = \mathbf{0}$. That is, each component of $\boldsymbol{x}$ remains stationary at $\mathbf{0}$ if $\boldsymbol{x}(0) = \mathbf{0}$. If, on the other hand, any one of the components of $\boldsymbol{x}$ is zero, then from system (10), it is easily seen that the differential equation corresponding to that component is non-negative and hence no trajectory of the system passes out of $\mathbb{R}^9_+$ through that component's zero axis. Next, to prove *positivity*, let the initial data

$$\boldsymbol{x}_0 = (E_a, G_{lM}, G_{lF}, G_M, G_F, Z, T, O, S)(0) \in \mathbb{R}^9_+.$$

Then we want to show that every solution $(E_a, G_{lM}, G_{lF}, G_M, G_F, Z, T, O, S)(t)$ is in $\mathbb{R}^9_+$ for all $t \geqslant 0$. To begin, let

$$t^* := \sup\{t > 0 \mid E_a(t) > 0,\ G_{lM}(t) > 0,\ G_{lF}(t) > 0,\ G_M(t) > 0, G_F(t) > 0,\ Z(t) > 0, T(t) > 0, O(t) > 0, S(t) > 0\}.$$

If $t^* = \infty$, then all solutions of the system are positive (from the definition of t^* as a least upper bound).

Suppose $t^* < \infty$, then by the definition of t^* there is $t < t^*$ such that at least one of $G_{lM}(t), G_{lF}(t), G_M(t), G_F(t), Z(t), T(t), O(t)$ or $S(t)$ is equal to zero at $t = t^*$. Let's check each individually. Suppose $E_a(t^*) = 0$ with

$$\begin{cases} E_a(t) > 0,\ G_{lM}(t) > 0,\ G_{lF}(t) > 0,\ G_M(t) > 0,\ G_F(t) > 0,\ Z(t) > 0, \\ T(t) > 0,\ O(t) > 0,\ S(t) > 0, \end{cases} \tag{13}$$

for $0 \leqslant t < t^*$. From (2), we have $E_a(t) = \tilde{E}_{a0} e^{-\tilde{\beta} t} \forall t \geqslant 0$, and thus $E_a(t) > 0, \forall t \geqslant 0$whenever $\tilde{E}_{a0} > 0$. This is a contradiction to the assumption that there is $t^* < \infty$ such that $E_a(t^*) = 0$. Hence, there is no such t^*. That is, $E_a(t) > 0,\ \forall t \geqslant 0$ provided that $\tilde{E}_{a0} > 0$. Next, suppose $G_{lM}(t^*) = 0$ with (14) satisfied. Then from the first equation of system (10), we have

$$G'_{lM}(t) = -c_1 G_{lM}(t), \text{with} G_{lM}(0) = \tilde{m} G_{l0}.$$

By separating variables and integrating we get

$$G_{lF}(t) = (1-\tilde{m}) G_{l0} e^{-d_1 t}, \forall t \geqslant 0, \tag{14}$$

and thus, $G_{lF}(t) = (1-\tilde{m}) G_{l0} e^{-d_1 t} > 0,\ \forall t \geqslant 0$, whenever $G_{lF}(0) = (1-\tilde{m}) G_{l0} > 0$. Hence, $G_{lF}(t) > 0, \forall t \geqslant 0$ provided that $G_{lF}(0) > 0$. Now, let $G_M(0) > 0$ and $G_M(t^*) = 0$, with (14) satisfied. Then from the third equation of model (10), we have

$$G'_M(t) + \left(a_1 + \frac{\beta_4 G_F(t)}{1+\xi E_a(t)}\right) G_M(t) = s_1 \tilde{\alpha}_1 c_1 G_{lM}(t) = s_1 \tilde{\alpha}_1 c_1 \tilde{m} G_{l0} e^{-c_1 t} \tag{15}$$

which is a first order linear ODE with integrating factor ($I.F$)

$$I.F = \exp\left(\int_0^t \left(a_1 + \frac{\beta_4 G_F(\tau)}{1+\xi E_a(\tau)}\right) d\tau\right).$$

Set

$$f_1(t) := s_1 \tilde{\alpha}_1 c_1 \tilde{m} G_{l0} e^{-c_1 t},\ u_1(t) = \exp\left(\int_0^t \left(a_1 + \frac{\beta_4 G_F(\tau)}{1+\xi E_a(\tau)}\right) d\tau\right). \tag{16}$$

Clearly $f_1(t) > 0$, and $u_1(t) > 0,\ \forall t \geqslant 0$ with $u_1(0) = 1$, $f_1(0) = s_1 \tilde{\alpha}_1 c_1 \tilde{m} G_{l0} > 0$. Now on multiplying (15) all through by its integrating factor $u_1(t)$, we get

$$u_1(t) \frac{dG_M}{dt} \left(a_1 + \frac{\beta_4 G_F(t)}{1+\xi E_a(t)}\right) u_1(t) G_M(t) = u_1(t) f_1(t).$$

Using product rule and then integrating from 0 to t^* yields,

$$G_M(t^*) = \frac{G_M(0)}{u_1(t^*)} + \frac{1}{u_1(t^*)} \int_0^{t^*} f_1(\tau) u_1(\tau) d\tau, \tag{17}$$

where $u_1(t)$ and $f_1(t)$ as given in (16). Since $u_1(t^*) > 0$, and $f_1(t^*) > 0$, for all $t^* \geqslant 0$, we have that $G_M(t^*) > 0, \forall t^* > 0$ whenever $G_M(0) > 0$. This contradicts our assumption that there is $t^* < \infty$ defined by (13) such that $G_M(t^*) = 0$. Hence, there is no such t^* such that $G_M(t^*) = 0$. Therefore, $G_M(t) > 0,\ \forall t \geqslant 0$ whenever the initial data is positive.

Alternatively, without solving for $G_M(t^*)$, we can show that $G_M(t^*) > 0, \forall t^* > 0$ whenever $G_M(0) > 0$. This is because the right hand side of (15), $f_1(t) := s_1 \tilde{\alpha}_1 c_1 \tilde{m} G_{l0} e^{-c_1 t}$, is always positive for all $t \geqslant 0$, and thus, we have

$$G'_M(t) + \left(a_1 + \frac{\beta_4 G_F(t)}{1+\xi E_a(t)}\right) G_M(t) > 0, \forall t \geqslant 0.$$

On multiplying all through out by the $u_1(t)$ as defined in (16), we have

$$\frac{d}{dt}(G_M(t) u_1(t)) > 0,\ \forall t \geqslant 0. \Rightarrow G_M(t) u_1(t)\big|_0^{t^*} > 0,\ \forall t \geqslant 0$$

This implies that $G_M(t^*) > \frac{G_M(0)}{u_1(t^*)}$ and hence, $G_M(t^*) > 0,\ \forall t^* > 0$ whenever $G_M(0) > 0$ since $u_1(t^*) > 0$, for all $t^* > 0$.

Next suppose $G_F(0) > 0$ and there is $t^* < \infty$ such that $G_F(t^*) = 0$ with (14) satisfied for $0 \leqslant t < t^*$. Then using the fourth equation of (10) and following similar steps as above, we arrive at

$$G_F(t^*) = \frac{G_F(0)}{u_2(t^*)} + \frac{1}{u_2(t^*)} \int_0^{t^*} f_2(\tau) u_2(\tau) d\tau, \tag{18}$$

where

$$u_2(t^*) = \exp\left(\int_0^{t^*} \left(b_1 + \frac{\beta_4 G_M(\tau)}{1+\xi E_a(\tau)}\right) d\tau\right) \text{ and } f_2(t^*) = v_1 \tilde{\alpha}_2 d_1 (1-\tilde{m}) G_{l0} e^{-d_1 t^*}. \tag{19}$$

This implies $G_F(t^*) > 0$ since $G_F(0) > 0$, which is a contradiction to the hypothesis that there is $t^* < \infty$ such that $G_F(t^*) = 0$. Hence, $G_F(t) > 0$, for all $t \geqslant 0$ whenever $G_F(0) > 0$.

Using similar methods, we can show that $G_F(t), Z(t), T(t), O(t)$ and $S(t)$ are positive for all $t \geqslant 0$ whenever their corresponding initial conditions are positive. Particularly, following similar steps, we get

$$Z(t^*) = \frac{Z(0)}{u_3(t^*)} + \frac{1}{u_3(t^*)} \int_0^{t^*} f_3(\tau) u_3(\tau) d\tau, \tag{20}$$

where

$$f_3(t) = \frac{\beta_4 G_M(t) G_F(t)}{1+\xi E_a(t)},\ u_3(t) = \exp\big((\mu_z + \delta_z) t\big). \tag{21}$$

$$T(t^*) = \frac{T(0)}{u_4(t^*)} + \frac{\delta_z}{u_4(t^*)} \int_0^{t^*} Z(\tau) u_4(\tau) d\tau, \tag{22}$$

where $u_4(t) = \exp\big((\mu_T + \delta_T) t\big)$.

$$O(t^*) = \frac{O(0)}{u_5(t^*)} + \frac{\delta_T}{u_5(t^*)} \int_0^{t^*} T(\tau) u_5(\tau) d\tau, \tag{23}$$

where $u_5(t^*) = \exp\left(\int_0^{t^*} (\mu_O + k(\tau) d\tau\right)$.

$$S(t^*) = \frac{S(0)}{u_6(t^*)} + \frac{n\tilde{p}}{u_6(t^*)} \int_0^{t^*} k(\tau) O(\tau) u_6(\tau) d\tau, \tag{24}$$

$u_6(t) = \exp(\mu_S t)$. Therefore, every forward solution of system (10) with positive initial data remains positive for $t \geqslant 0$.

It guarantees that non-negative solutions are obtained only when an initial positive number of mature gametocytes or adap-

tive immune cells are ingested with a blood meal taken by a female feeding anopheles mosquitoes.

Theorem 2. [Boundedness of solution] *Consider system (10) with initial conditions Eq. (11). Then every forward solution of the system in $\mathbb{R}^9_+$ with initial condition in $\mathbb{R}^9_+$ remains bounded. Furthermore, any solution of the model system (10) starting in $\mathbb{R}^9_+$ eventually remains in the region $\Omega_v \subset \mathbb{R}^9_+$ defined by:*

$$\Omega_v := \left\{ \begin{array}{l} (E_a, G_{IM}, G_{IF}, G_M, G_F, Z, T, O, S) \in \mathbb{R}^9_+ : 0 \leqslant E_a \leqslant \widetilde{E}_{a0},\ 0 \leqslant G_{IM} \leqslant \tilde{m}G_{I0}, \\ 0 \leqslant G_{IF} \leqslant (1-\tilde{m})G_{I0},\ 0 \leqslant G_M \leqslant G_M^{\infty},\ 0 \leqslant G_F \leqslant G_F^{\infty},\ 0 \leqslant Z \leqslant Z^{\infty}, \\ 0 \leqslant T \leqslant T^{\infty},\ 0 \leqslant O \leqslant O^{\infty},\ 0 \leqslant S \leqslant S^{\infty}, \end{array} \right\} \tag{25}$$

where, $G_M^{\infty}, G_F^{\infty}, Z^{\infty}, T^{\infty}, O^{\infty}$ and S^{∞} are the respective upper bounds of G_M, G_F, Z, T, O and S given by $G_M^{\infty} = \frac{s_1\tilde{\alpha}_1 c_1 \tilde{m} G_{I0}}{a_1}, G_F^{\infty} = \frac{\nu_1 \tilde{\alpha}_2 d_1 (1-\tilde{m}) G_{I0}}{b_1}, Z^{\infty} = \frac{\beta_4 G_M^{\infty} G_F^{\infty}}{\mu_z + \delta_z}, T^{\infty} = \frac{\delta_z Z^{\infty}}{\mu_T + \delta_T}, O^{\infty} = \frac{\delta_T T^{\infty}}{\delta_T}$ and $S^{\infty} = \frac{\tilde{a}n\tilde{p}O^{\infty}}{\mu_s}$.

Proof of Theorem 2 (Boundedness of solution):

Recall that $0 < E_a(t) \leqslant \widetilde{E}_{a0},\ \forall t \geqslant 0$. Thus, $E_a(t)$ is bounded for all $t \geqslant 0$. Next to show the boundedness of G_{IM} and G_{IF}, we have

$$G_{IM}(t) = \tilde{m}G_{I0}e^{-c_1 t},\ G_{IF}(t) = (1-\tilde{m})G_{I0}e^{-d_1 t}.$$

It is easily seen that G_{IM} and G_{IM} are continuous decreasing functions of time t satisfying $G_{IM}(t) \to 0$ and $G_{IF}(t) \to 0$ as $t \to \infty$. Thus, $G_{IM}(t)$ and $G_{IF}(t)$ are bounded components of the solution vector of system (10) for all $t \geqslant 0$, satisfying

$$0 \leqslant G_{IM}(t) \leqslant \tilde{m}G_{I0},\ 0 \leqslant G_{IF}(t) \leqslant (1-\tilde{m})G_{I0}, \forall t \geqslant 0. \tag{26}$$

Now considering the equation of G_M':

$$\frac{dG_M}{dt} = s_1\tilde{\alpha}_1 c_1 G_{IM} - a_1 G_M - \frac{\beta_4 G_M G_F}{1+\xi E_a} \leqslant s_1\tilde{\alpha}_1 c_1 G_{IM} - a_1 G_M$$
$$\leqslant s_1\tilde{\alpha}_1 c_1 \tilde{m} G_{I0} - a_1 G_M, \text{ by (26)}, \Rightarrow \frac{dG_M}{dt} + a_1 G_M \leqslant s_1\tilde{\alpha}_1 c_1 \tilde{m} G_{I0}.$$

Now integrating using the integration factor $e^{a_1 t}$ yields

$$G_M(t) \leqslant \frac{s_1\tilde{\alpha}_1 c_1 \tilde{m} G_{I0}}{a_1} + A_1 e^{-a_1 t}, \forall t \geqslant 0,$$

where A_1 is an arbitrary constant that can be determined using the initial data. Observe that if the initial condition $G_M(0) > \frac{s_1\tilde{\alpha}_1 c_1 \tilde{m} G_{I0}}{a_1}$, then $A_1 > 0$ and the bound for $G_M(t)$ is decreasing with time. If $G_M(0) = \frac{s_1\tilde{\alpha}_1 c_1 \tilde{m} G_{I0}}{a_1}$, then $A_1 \geqslant 0$ and the bound for $G_M(t)$ is non-increasing with time. Finally, if $G_M(0) < \frac{s_1\tilde{\alpha}_1 c_1 \tilde{m} G_{I0}}{a_1}$, then $A_1 < 0$ and the bound for $G_M(t)$ will be an increasing function of t. In any of the instances we see that as $t \to \infty, G_M(t) \leqslant \frac{s_1\tilde{\alpha}_1 c_1 \tilde{m} G_{I0}}{a_1}$. So, we have

$$\limsup_{t\to\infty} G_M(t) \leqslant \frac{s_1\tilde{\alpha}_1 c_1 \tilde{m} G_{I0}}{a_1}.$$

Thus, by definition of lim sup there exists $\epsilon_1 > 0$, such that

$$0 \leqslant G_M(t) \leqslant \frac{s_1\tilde{\alpha}_1 c_1 \tilde{m} G_{I0}}{a_1} + \epsilon_1, \forall t \geqslant 0. \tag{27}$$

So there exist $0 \leqslant G_M^{\infty} = \frac{s_1\tilde{\alpha}_1 c_1 \tilde{m} G_{I0}}{a_1} < \infty$ such that

$$0 \leqslant G_M(t) \leqslant G_M^{\infty},\ \forall t \geqslant 0. \tag{28}$$

Hence, $G_M(t)$ is a bounded component of the solution vector of system (10), for all $t \geqslant$.

Similarly, we can show that $\lim_{t\to\infty}\sup G_F(t) \leqslant \frac{\nu_1\tilde{\alpha}_2 d_1(1-\tilde{m})G_{I0}}{b_1}$, $\lim_{t\to\infty}\sup Z(t) \leqslant \frac{\beta_4 G_M^{\infty} G_F^{\infty}}{\mu_z+\delta_z}$, $\lim_{t\to\infty}\sup T(t) \leqslant \frac{\delta_z Z^{\infty}}{\mu_T+\delta_T}$, $\lim_{t\to\infty}\sup O(t) \leqslant \frac{\delta_T T^{\infty}}{\delta_T}$ and $\lim_{t\to\infty}\sup S(t) \leqslant \frac{\tilde{a}n\tilde{p}O^{\infty}}{\mu_s}$, where we used $k(t) \leqslant \tilde{a} < \infty$, for all $t \geqslant 0$ since $k(t)$ given in (8) is a bounded non-negative function of t.

Therefore, each forward solution is bounded with upper bounds $E_a^{\infty} = \widetilde{E}_{a0}, G_{IM}^{\infty} = \tilde{m}G_{I0}, G_{IF}^{\infty} = (1-\tilde{m})G_{I0}, G_M^{\infty} = \frac{s_1\tilde{\alpha}_1 c_1 \tilde{m} G_{I0}}{a_1}, G_F^{\infty} = \nu_1 \frac{\tilde{\alpha}_2 d_1 (1-\tilde{m}) G_{I0}}{b_1}, Z^{\infty} = \frac{\beta_4 G_M^{\infty} G_F^{\infty}}{\mu_z+\delta_z}, T^{\infty} = \frac{\delta_z Z^{\infty}}{\mu_T+\delta_T}, O^{\infty} = \frac{\delta_T T^{\infty}}{\delta_T}$ and $S^{\infty} = \frac{\tilde{a}n\tilde{p}O^{\infty}}{\mu_s}$. Moreover, the set Ω_v defined in (25) is positively invariant.

Theorem 3 (*Uniqueness of solution*). *Model (10) which is written as an initial value problem in Eq. (12) has a unique non-negative solution which remains bounded.*

Proof of Theorem 3 (Uniqueness of solution):

We use the Picard-Cauchy-Lipschitz theorem for existence and uniqueness of solution, see Hsieh and Sibuya, 2012. Thus, we are required to show that the right hand side function Φ is $\mathscr{C}^1$ and Lipschitz in $U \times [0, T]$ where $U \subset \mathbb{R}^9_+$ is an open set and $[0, T] \subset [0, \infty)$. But it is known from theory of ordinary differential equations that to show that Φ is Lipschitz continuous, it suffices to show that the partial derivative $\frac{\partial\Phi}{\partial x_i}$ exists, continuous and bounded, $\forall i = 0, 1, 2, \cdots, 8$ where $(x_0, x_1, x_2, x_3, x_4, x_5, x_6, x_7, x_9) = (E_a, G_{IM}, G_{IF}, G_M, G_F, Z, T, O, S)$.

We recall that every differentiable function is continuous. From the first equation of (10), we observe that $\phi_0(x) = -\tilde{\beta}E_a$ is continuous since it is a constant multiple of a differentiable function E_a. Similarly, $\phi_1(x) = -c_1 G_{IM}$ is continuous, so does G_{IF}. From the third equation of (10), $\phi_3 = s_1\tilde{\alpha}_1 c_1 G_{IM} - a_1 G_M - \frac{\beta_4 G_M G_F}{1+\xi E_a}$, is a linear combination of a constant (continuous) and differentiable functions $G_{IM}(t), G_M(t), G_M$, $G_F(t)$ and $E_a(t)$. Hence, ϕ_3 is continuous since any linear combination of continuous terms is also continuous.

Similarly, $\phi_4(x), \cdots, \phi_8(x)$ are linear combination of differentiable functions (continuous) and therefore they are all continuous. We next show that for each $i = 0, 1, \cdots, 8, \frac{\partial\Phi}{\partial x_i}$ is continuous and bounded. But $\frac{\partial\Phi}{\partial x_i}$ is continuous if each $\frac{\partial\phi_j}{\partial x_i}$ is continuous $\forall i, j = 0, 1, \cdots, 8$. We next show that each function $\phi_j, j = 0, 1, \cdots, 8$ in the right had side of (10) is $\mathscr{C}^1$, that is, $\frac{\partial\phi_j}{\partial x_i}$ is continuous.

It is to show that $\frac{\partial\phi_j}{\partial x_i}$ exists and are continuous and hence $\Phi \in \mathscr{C}^1$ since each partial derivatives consist of constants and continuous functions.

Next we show that $\frac{\partial\Phi}{\partial x}$ is bounded, that is, $\|\frac{\partial\Phi}{\partial x}\|_{\infty}$ is bounded for $x = (E_a, G_{IM}, G_{IF}, G_M, G_F, Z, T, O, S)$, where $\frac{\partial\Phi}{\partial x} = \frac{\partial}{\partial x_i}\begin{pmatrix}\phi_0,\\ \phi_1\\ \vdots\\ \phi_8\end{pmatrix}$, $i = 0, 1, 2, \cdots, 8$.

Using maximum norm, we have

$$\|\frac{\partial\Phi}{\partial E_a}\|_{\infty} = \max\left\{|-\tilde{\beta}|, |0|, |0|, |-\frac{\beta_4\xi G_M G_F}{(1+\xi E_a)^2}|, |-\frac{\beta_4\xi G_M G_F}{(1+\xi E_a)^2}|, |\frac{\beta_4\xi G_M G_F}{(1+\xi E_a)^2}|, |0|, |0|, |0|\right\} < \infty,$$

since we have already proved that $G_M(t)$ and $G_F(t)$ are bounded for all $t \geqslant 0$.

Continuing to the next component, we have

$$\frac{\partial\Phi}{\partial G_{IM}} = \frac{\partial}{\partial G_{IM}}\begin{pmatrix}\phi_1\\ \vdots\\ \phi_8\end{pmatrix} = (0, -c_1, 0, 0, 0, 0, 0, 0, 0)^{Tr}$$

Using the maximum norm, we get

$$\|\frac{\partial \Phi}{\partial G_{IM}}\|_\infty = \max\{|0|, |-c_1|, |0|, |0|, |0|, |0|, |0|, |0|, |0|\} = c_1 < \infty.$$

Similarly,

$$\|\frac{\partial \Phi}{\partial G_{IF}}\|_\infty = \max\{|0|, |-d_1|, |0|, |0|, |0|, |0|, |0|, |0|, |0|\} = d_1 < \infty,$$

$$\|\frac{\partial \Phi}{\partial G_{M}}\|_\infty = \max\left\{|0|, |0|, |-a_1 - \frac{\beta_4 G_F}{1+\xi E_a}|, |-\frac{\beta_4 G_F}{1+\xi E_a}|, |\frac{\beta_4 G_F}{1+\xi E_a}|, |0|, |\delta_T|, |0|\right\} < \infty.$$

Similarly, we can compute the remaining norms and we obtain $\|\frac{\partial \Phi}{\partial x_i}\|_\infty$ for each $x_i \in \{G_F, Z, T, O, S\}$. Therefore, we conclude that $\frac{\partial \Phi}{\partial x}$ is bounded for all variables $x = (E_a, G_{IM}, G_{IF}, G_M, G_F, Z, T, O, S)$. Since $\frac{\partial \Phi}{\partial x}$ exists, is continuous and bounded, Φ is Lipschitz continuous, then by the existence and uniqueness theorem, model (10) has a unique solution.

While proving the positivity of solution in Theorem 1, we also have showed the lemma. The general solution to system (10) is given below in the next lemma.

Lemma 1 (*General Solution of System (10)*). *The unique non-negative bounded solution,* $(E_a(t), G_{IM}(t), G_{IF}(t), G_M(t), G_F(t), Z(t), T(t), O(t), S(t))^{Tr} \in \mathbb{R}^9_+$, *of system (10) with initial condition in (11) at any* $t \geqslant 0$ *is given as:*

$$\begin{cases} E_a(t) = \tilde{E}_{a0} e^{-\tilde{\beta} t}, G_{IM}(t) = \tilde{m} G_{I0} e^{-c_1 t}, G_{IF}(t) = (1-\tilde{m}) G_{I0} e^{-d_1 t}, \\ G_M(t) = \frac{1}{u_1(t)} \int_0^t f_1(\tau) u_1(\tau) d\tau, \ G_F(t) = \frac{1}{u_2(t)} \int_0^t f_2(\tau) u_2(\tau) d\tau, \\ Z(t) = \frac{1}{u_3(t)} \int_0^t f_3(\tau) u_3(\tau) d\tau, \ T(t) = \frac{\delta_z}{u_4(t)} \int_0^t Z(\tau) u_4(\tau) d\tau, \\ O(t) = \frac{\delta_T}{u_5(t)} \int_0^t T(\tau) u_5(\tau) d\tau, \ S(t^*) = \frac{n\bar{p}}{u_6(t^*)} \int_0^{t^*} k(\tau) O(\tau) u_6(\tau) d\tau, \end{cases} \tag{29}$$

where,

$$f_1(t) := s_1 \tilde{\alpha}_1 c_1 \tilde{m} G_{I0} e^{-c_1 t}, \ f_2(t) = v_1 \tilde{\alpha}_2 d_1 (1-\tilde{m}) G_{I0} e^{-d_1 t}, \ f_3(t) = \frac{\beta_4 G_M(t) G_F(t)}{1 + \xi E_a(t)},$$

and

$$u_1(t) = \exp\left(\int_0^t \left(a_1 + \frac{\beta_4 G_F(\tau)}{1+\xi E_a(\tau)}\right) d\tau\right), u_2(t^*) = \exp\left(\int_0^{t^*} \left(b_1 + \frac{\beta_4 G_M(\tau)}{1+\xi E_a(\tau)}\right) d\tau\right),$$
$$u_3(t) = \exp((\mu_z + \delta_z)t), \ u_4(t) = \exp((\mu_T + \delta_T)\tau),$$
$$u_5(t) = \exp\left(\int_0^t (\mu_O + k(\tau) d\tau\right), \ u_6(t) = \exp(\mu_S t)\Big\}.$$

References

Acquah, F.K., Adjah, J., Williamson, K.C., Amoah, L.E., 2019. Transmission-blocking vaccines: old friends and new prospects. Infect. Immun. 87 (6), e00775–18.

Aikawa, Masamichi, Rener, Joan, Carter, Richard, Miller, Louis H., 1981. An electron microscopical study of the interaction of monoclonal antibodies with gametes of the malarial parasite plasmodium gallinaceum. J. Eukaryot. Microbiol. 28 (3), 383–388.

Aly, Ahmed S.I., Vaughan, Ashley M., Kappe, Stefan H.I., 2009. Malaria parasite development in the mosquito and infection of the mammalian host. Annu. Rev. Microbiol. 63, 195–221.

Anguelov, Roumen, Dumont, Yves, Lubuma, Jean, 2012. Mathematical modeling of sterile insect technology for control of anopheles mosquito. Comput. Math. Appl. 64 (3), 374–389.

Arévalo-Herrera, Myriam, Solarte, Yezid, Marin, Catherin, Santos, Mariana, Castellanos, Jenniffer, Beier, John C., Valencia, Sócrates Herrera, 2011. Malaria transmission blocking immunity and sexual stage vaccines for interrupting malaria transmission in latin america. Memórias do Instituto Oswaldo Cruz 106, 202–211..

Augustine, Alison Deckhut, Fenton Hall, B., Leitner, Wolfgang W., Mo, Annie X., Wali, Tonu M., Fauci, Anthony S., 2009. Niaid workshop on immunity to malaria: addressing immunological challenges. Nat. Immunol. 10 (7), 673–678.

Ballou, W.R., 2009. The development of the rts, s malaria vaccine candidate: challenges and lessons. Parasite Immunol. 31 (9), 492–500.

Baton, Luke A., Ranford-Cartwright, Lisa C, 2005. Spreading the seeds of million-murdering death: metamorphoses of malaria in the mosquito. Trends Parasitol. 21 (12), 573–580.

Beier, John C., 1998. Malaria parasite development in mosquitoes. Annu. Rev. Entomol. 43 (1), 519–543.

Bennink, Sandra, Kiesow, Meike J., Pradel, Gabriele, 2016. The development of malaria parasites in the mosquito midguto. Cell. Microbiol. 18 (7), 905–918.

Sumi Biswas, 2017. Can we block malaria transmission.https://www.ndm.ox.ac.uk/sumi-biswas-can-we-block-malaria-transmission. Accessed: Agust 27, 2017..

Blagborough, A.M., Churcher, T.S., Upton, L.M., Ghani, A.C., Gething, P.W., Sinden, R. E., 2012. Transmission-blocking interventions eliminate malaria from laboratory populations. Nat. Commun. 4 (9), 1812.

Bousema, J.T., Drakeley, C.J., Kihonda, J., Endriks, J.C.M., Akim, N.I.J., Roeffen, W., Sauerwein, R.W., 2007. A longitudinal study of immune responses to plasmodium falciparum sexual stage antigens in tanzanian adults. Parasite Immunol. 29 (6), 309–317.

Bousema, T., Sutherland, C.J., Churcher, T.S., Mulder, B., Gouagna, L.C., Riley, E.M., Targett, G.A., Drakeley, C.J., 2011. Human immune responses that reduce the transmission of plasmodium falciparum in african populations. Int. J. Parasitol. 41 (3–4), 293–300.

Bousema, Teun, Sutherland, Colin J., Churcher, Thomas S., Mulder, Bert, Gouagna, Louis C., Riley, Eleanor M., Targett, Geoffrey A.T., Drakeley, Chris J., 2011. Human immune responses that reduce the transmission of plasmodium falciparum in african populations. Int. J. Parasitol. 41 (3), 293–300.

Carter, Richard, 2001. Transmission blocking malaria vaccines. Vaccine 19 (17), 2309–2314.

CDC, 2015. Anopheles mosquitoes.https://www.cdc.gov/malaria/about/biology/mosquitoes/. Reviewed and updated: October 21, 2015, Last Accessed: August 30, 2017..

Chaturvedi, Neha, Bharti, Praveen K., Tiwari, Archana, Singh, Neeru, 2016. Strategies & recent development of transmission-blocking vaccines against plasmodium falciparum. Indian J. Med. Res. 143 (6), 696.

Childs, Lauren M., Prosper, Olivia F., 2017. Simulating within-vector generation of the malaria parasite diversity. PloS One 12, (5) e0177941.

Churcher, Thomas S., Blagborough, Andrew M., Delves, Michael, Ramakrishnan, Chandra, Kapulu, Melissa C., Williams, Andrew R., Biswas, Sumi, Da, Dari F., Cohuet, Anna, Sinden, Robert E., 2012. Measuring the blockade of malaria transmission–an analysis of the standard membrane feeding assay. Int. J. Parasitol. 42 (11), 1037–1044.

Churcher, Thomas S., Sinden, Robert E., Edwards, Nick J., Poulton, Ian D., Rampling, Thomas W., Brock, Patrick M., Griffin, Jamie T., Upton, Leanna M., Zakutansky, Sara E., Sala, Katarzyna A., et al., 2017. Probability of transmission of malaria from mosquito to human is regulated by mosquito parasite density in naive and vaccinated hosts. PLoS Pathogens 13, (1) e1006108.

Coalson, Jenna E., Walldorf, Jenny A., Cohee, Lauren M., Ismail, Miriam D., Mathanga, Don, Cordy, Regina Joice, Marti, Matthias, Taylor, Terrie E., Seydel, Karl B., Laufer, Miriam K., Wilson, Mark L., 2016. High prevalence of plasmodium falciparum gametocyte infections in school-age children using molecular detection: patterns and predictors of risk from a cross-sectional study in southern malawi. Malaria J. 15 (1), 527.

Da, Dari F., Churcher, Thomas S., Yerbanga, Rakiswendé S., Yaméogo, Bienvenue, Sangaré, Ibrahim, Ouedraogo, Jean Bosco, Sinden, Robert E., Blagborough, Andrew M., Cohuet, Anna, 2015. Experimental study of the relationship between plasmodium gametocyte density and infection success in mosquitoes; implications for the evaluation of malaria transmission-reducing interventions. Exp. Parasitol. 149, 74–83.

de Jong, R.M., Tebeje, S.K., MeersteinKessel, L., Tadesse, F.G., Jore, M.M., Will Stone, W., Bousema, T., 2020. Immunity against sexual stage plasmodium falciparum and plasmodium vivax parasites. Immunol. Rev. 293 (1), 190–215.

Delves, M.J., Angrisano, F., Blagborough, A.M., 2018. Antimalarial transmission-blocking interventions: past, present, and future. Trends Parasitol. 34 (9), 735–746.

Dhar, Ravi, Kumar, Nirbhay, 2003. Role of mosquito salivary glands. Curr. Sci.-Bangalore 85 (9), 1308–1313.

Doumbo, Ogobara K., Niaré, Karamoko, Healy, Sara A., Sagara, Issaka, Duffy, Patrick E., 2018. Malaria transmission-blocking vaccines: present status and future perspectives. Towards Malaria Elimination-A Leap Forward.

Draper, S.J., Sack, B.K., King, C.R., Nielsen, C.M., Rayner, J.C., Higgins, M.K., Long, C.A., Seder, R.A., 2018. Malaria vaccines: recent advances and new horizons. Cell Host Microbe 24 (1), 43–56.

Gardiner, Donald L., Trenholme, Katharine R., 2015. Plasmodium falciparum gametocytes: playing hide and seek. Ann. Transl. Med. 3(4)..

Gazzinelli, Ricardo T., Kalantari, Parisa, Fitzgerald, Katherine A., Golenbock, Douglas T., 2014. Innate sensing of malaria parasites. Nat. Rev. Immunol. 14 (11), 744–757.

Graves, Patricia M., Gelband, Hellen, 2016. Vaccines for preventing malaria (pre-erythrocytic)). The Cochrane Database Syst. Rev. 4, CD006198..

Hamby, D.M., 1994. A review of techniques for parameter sensitivity analysis of environmental models. Environ. Monit. Assessment 32 (2), 135–154.

Hay, S.I., Smith, D.L., Snow, R.W., 2008. Measuring malaria endemicity from intense to interrupted transmission. Lancet Infect. Dis. 84 (6), 369–378.

Hill, Adrian V.S., 2011. Vaccines against malaria. Philos. Trans. R. Soc. B 366 (1579), 2806–2814.

Holz, Lauren E., Fernandez-Ruiz, Daniel, Heath, William R., 2016. Protective immunity to liver-stage malaria. Clin. Transl. Immunol. 5, e105.

Hsieh, Po-Fang, Sibuya, Yasutaka, 2012. Basic Theory of Ordinary Differential Equations. Springer Science & Business Media.

Kapulu, Melissa C., Biswas, Sumi, Blagborough, Andrew, Gilbert, Sarah C., Sinden, Robert E., Hill, Adrian V.S., 2010. Viral vectored transmission blocking vaccines against plasmodium falciparum. Malaria J. 9 (2). O22.
Kaslow, David C., 1993. Transmission-blocking immunity against malaria and other vector-borne diseases. Curr. Opin. Immunol. 5 (4), 557–565.
Kaushal, D.C., Carter, R., Miller, L.H., Krishna, G., 1980. Gametocytogenesis by malaria parasites in continuous culture. Nature 286 (5772), 490–492.
Kengne-Ouafo, Jonas A., Sutherland, Colin J., Binka, Fred N., Awandare, Gordon A., Urban, Britta C., Dinko, Bismarck, 2019. Immune responses to the sexual stages of plasmodium falciparum parasites. Front. Immunol. 10, 136.
Klein, E., Smith, D., Boni, M.F., Laxminarayan, R., 2008. Clinically immune hosts as a refuge for drug-sensitive malaria parasites. Malar J. 7 (1), 67.
Krettli, Antoniana U., Miller, Louis H., 2001. Malaria: a sporozoite runs through it. Curr. Biol. 11 (10), R409–R412.
Kuehn, Andrea, Pradel, Gabriele, 2010. The coming-out of malaria gametocytes. BioMed Res. Int. 2010.
Laurens, Matthew B., 2020. RTS, S/AS01 vaccine (Mosquirix): an overview. Human Vaccines Immunotherap. 16 (3), 480–489.
Manore, Carrie A., Teboh-Ewungkem, Miranda I., Prosper, Olivia, Peace, Angela, Gurski, Katharine, Feng, Zhilan, 2019. Intermittent preventive treatment (ipt): Its role in averting disease-induced mortality in children and in promoting the spread of resistance spread in areas with population movement antimalarial drug resistance. Bull. Math. Biol. 81, 193–234.
McQueen, Philip G., Williamson, Kim C., Ellis McKenzie, F., 2013. Host immune constraints on malaria transmission: insights from population biology of within-host parasites. Malaria J. 12 (1).
Mueller, Ann-Kristin, Kohlhepp, Florian, Hammerschmidt, Christiane, Michel, Kristin, 2010. Invasion of mosquito salivary glands by malaria parasites: prerequisites and defense strategies. Int. J. Parasitol. 40 (11), 1229–1235.
MVI PATH, 2017. The rts, s malaria vaccine candidate.http://www.malariavaccine.org/sites/www.malariavaccine.org/files/content/page/files/mviCVIA_rtss.pdf. **Published: April 2017, Accessed: November, 2017..**
Ngwa, Gideon A., 2006. On the population dynamics of the malaria vector. Bull. Math. Biol. 68 (8), 2161–2189.
Ngwa, Gideon A., Shu, William S., 2000. A mathematical model for endemic malaria with variable human and mosquito populations. Math. Comput. Model. 32 (7–8), 747–764.
Ngwa, Gideon A., Teboh-Ewungkem, Miranda I., 2016. A mathematical model with quarantine states for the dynamics of ebola virus disease in human populations. Comput. Math. Methods Med.
Ngwa, Gideon A., Wankah, Terence T., Fomboh-Nforba, Mary Y., Ngonghala, Calsitus N., Teboh-Ewungkem, Miranda I., 2014. On a reproductive stage-structured model for the population dynamics of the malaria vector. Bull. Math. Biol. 76, 2476–2516.
Ngwa, Gideon A., Teboh-Ewungkem, Miranda I., Dumont, Yves, Ouifki, Rachid, Banasiak, Jacek, 2019. On a three-stage structured model for the dynamics of malaria transmission with human treatment, adult vector demographics and one aquatic stage. Theor. Biol. 481 (21), 202–222.
Ngwa, Gideon A., Woldegerima, Woldegebriel A., Teboh-Ewungkem, Miranda I., 2020. A mathematical study of the implicit role of innate and adaptive immune responses on within-human plasmodium falciparum parasite levels. J. Biol. Syst. 28 (2), 377–429.
Nunes, Julia K., Woods, Colleen, Carter, Terrell, Raphael, Theresa, Morin, Merribeth J., Diallo, Diadier, Leboulleux, Didier, Jain, Sanjay, Loucq, Christian, Kaslow, David C., et al., 2014. Development of a transmission-blocking malaria vaccine: progress, challenges, and the path forward. Vaccine 32 (43), 5531–5539.
Ouédraogo, A.L., Bousema, T., de Vlas, S.J., Cuzin-Ouattara, N., Verhave, J.P., Drakeley, C., Luty, A.J., Sauerwein, R., 2010. The plasticity of plasmodium falciparum gametocytaemia in relation to age in burkina faso. Malar. J. 9, 281.
Ouédraogo, A.L., Roeffen, W., Luty, S.J., sde Vlas, A.J., Nebie, I., Ilboudo-Sanogo, E., Cuzin-Ouattara, N., Teleen, K., Tiono, A.B., Sirima, S.B., Verhave, J.P., Bousema, T., Sauerwein, R., 2011. Naturally acquired immune responses to plasmodium falciparum sexual stage antigens pfs48/45 and pfs230 in an area of seasonal transmission. Infect. Immun. 79 (12), 4957–4964.
Pichon, Gaston, Awono-Ambene, H.P., Robert, Vincent, 2000. High heterogeneity in the number of plasmodium falciparum gametocytes in the bloodmeal of mosquitoes fed on the same host. Parasitology 121 (2), 115–120.
Rener, J., Carter, R., Rosenberg, Y., Miller, L.H., 1980. Anti-gamete monoclonal antibodies synergistically block transmission of malaria by preventing fertilization in the mosquito. Proc. Natl. Acad. Sci. U.S.A. 77 (11), 6797–6799.
Rodriguez-Barraquer, I., Arinaitwe, E., Jagannathan, P., Kamya, M.R., Rosenthal, P.J., Rek, J., Dorsey, G., Nankabirwa, J., Staedke, S.G., Kilama, M., Drakeley, C., Ssewanyana, Smith, D.L., Greenhouse, B., 2018. Quantification of anti-parasite and anti-disease immunity to malaria as a function of age and exposure. Elife 7, e35832.
Sauerwein, R.W., Bousema, T., 2015. Transmission blocking malaria vaccines: assays and candidates in clinical development. Vaccine 33 (52), 7476–7482.
Saul, A., 2008. Efficacy model for mosquito stage transmission blocking vaccines for malaria. Parasitology 135 (13), 1497–1506.
Sinden, Robert, 2010. A biologist's perspective on malaria vaccine development. Human Vaccines 6 (1), 3–11.
Sinden, Robert E., 2017. Developing transmission-blocking strategies for malaria control. PLoS Pathogens 13(7).
Tavares, J.C., 2013. Malaria. Colloquium Series on Integrated Systems Physiology: From Molecule to Function. Biota Publishing..
Teboh-Ewungkem, Miranda I., Yuster, Thomas, Newman, Nathaniel H., 2010. A mathematical model of the within-vector dynamics of the plasmodium falciparum protozoan parasite..
Teboh-Ewungkem, Miranda I., Wang, Miao, 2012. Male fecundity and optimal gametocyte sex ratios for plasmodium falciparum during incomplete fertilization. J. Theor. Biol. 307, 183–192.
Teboh-Ewungkem, Miranda I., Yuster, Thomas, 2010. A within-vector mathematical model of plasmodium falciparum and implications of incomplete fertilization on optimal gametocyte sex ratio. J. Theor. Biol. 264 (2), 273–286.
Teboh-Ewungkem, Miranda I., Yuster, Thomas, 2016. Evolutionary implications for the determination of gametocyte sex ratios under fecundity variation for the malaria parasite. J. Theor. Biol. 408, 260–273.
Teboh-Ewungkem, Miranda I., Ngwa, Gideon A., Ngonghala, Calistus N., 2013. Models and proposals for malaria: a review. Math. Popul. Stud. 20 (2), 57–81.
Teboh-Ewungkem, Miranda I., Mohammed-Awel, Jemal, Baliraine, Frederick N., Duke-Sylvester, Scott M., 2014. The effect of intermittent preventive treatment on anti-malarial drug resistance spread in areas with population movement. Malar. J. 13 (1), 428.
Teboh-Ewungkem, Miranda I., Prosper, Olivia, Gurski, Katharine, Manore, Carrie A., Peace, Angela, Feng, Zhilan, 2015. Intermittent preventive treatment (ipt) and the spread of drug resistant malaria. In: Applications of Dynamical Systems in Biology and Medicine. Springer, pp. 197–233.
Teboh-Ewungkem, Miranda I., Ngwa, Gideon A., Fomboh-Nforba, Mary Y., 2019. A multistage mosquito-centered mathematical model for malaria dynamics that captures mosquito gonotrophic cycle contributions to its population abundance and malaria transmission..
Valupadasu, Manasa, Mateti, Uday, 2012. Advanced malarial vaccines: a promising approach in the treatment of malaria. Syst. Rev. Pharmacy 3 (1), 31.
Vinetz, J.M., 2005. Plasmodium ookinete invasion of the mosquito midgut. In: Compans, R.W. et al. (Eds.), Malaria: Drugs, Disease and Post-genomic Biology, Current Topics in Microbiology and Immunology, vol. 295. Springer, Berlin, Heidelberg, pp. 357–382.
Wadi, Ishan, Anvikar, Anupkumar R., Mahendra Nath, C., Pillai, Radhakrishna, Sinha, Abhinav, Valecha, Neena, 2018. Critical examination of approaches exploited to assess the effectiveness of transmission-blocking drugs for malaria. Future Med. Chem. 10 (22), 2619–2639.
Wang, Claire Y.T., McCarthy, James S., Stone, Will J., Bousema, Teun, Collins, Katharine A., Bialasiewicz, Seweryn, 2018. Assessing plasmodium falciparum transmission in mosquito-feeding assays using quantitative pcr. Malar. J. 17 (1), 249.
WHO, 2017. World Malaria Report 2017. World Health Organization (WHO)..
WHO, 2020. Malaria vaccines.https://www.who.int/immunization/research/development/malaria/en/. **Last Accessed: May 27, 2020..**
Woldegerima, Wodegebriel Assefa, 2018. Mathematical Modeling of the Immunopathogenesis of the Within Human Host and the Within Vector Host Dynamics of the Malaria Parasite (Ph.D. thesis). Department of Mathematics, University of Buea, Cameroon..
Woldegerima, Woldegebriel A., Ngwa, Gideon A., Teboh-Ewungkem, Miranda I., 2018. Sensitivity analysis for a within-human-host immuno-pathogenesis dynamics of plasmodium falciparum parasites. Texts Biomath. 1, 140–168.
Woldegerima, Woldegebriel A., Teboh-Ewungkem, Miranda I., Ngwa, Gideon A., 2019. The impact of recruitment on the dynamics of an immune-suppressed within-human–host model of the plasmodium falciparum parasite. Bull. Math. Biol. 81 (11), 4564–4619.
Wu, Jianyong, Dhingra, Radhika, Gambhir, Manoj, Remais, Justin V., 2013. Sensitivity analysis of infectious disease models: methods, advances and their application. J. R. Soc. Interface 10 (86). 20121018.